

ANPC 2019,  
Kruger National Park, RSA

# Helium Decays of Excited States and Clustering in $^{17,18}\text{O}$

Neven Soić

Ruđer Bošković Institute Zagreb, Croatia



# Collaborators

L. Prepolec, L. Grassi, D. Jelavić Malenica, T. Mijatović, Đ. Miljanić, N. Skukan,  
S. Szilner, V. Tokić, M. Uroić

***Ruđer Bošković Institute, Zagreb, Croatia***

M. Milin

***Faculty of Science, University of Zagreb, Croatia***

S. Bailey, M. Freer, D. J. Marin-Lambarri, Tz. Kokalova Wheldon, J. Walshe, C. Wheldon  
***School of Physics and Astronomy, University of Birmingham, UK***

M. Fisichella, A. Di Pietro, P. Figuera, M. Lattuada, V. Scuderi  
***INFN –Laboratori Nazionali del Sud, Catania, Italy***

J. Gibelin, N. Orr

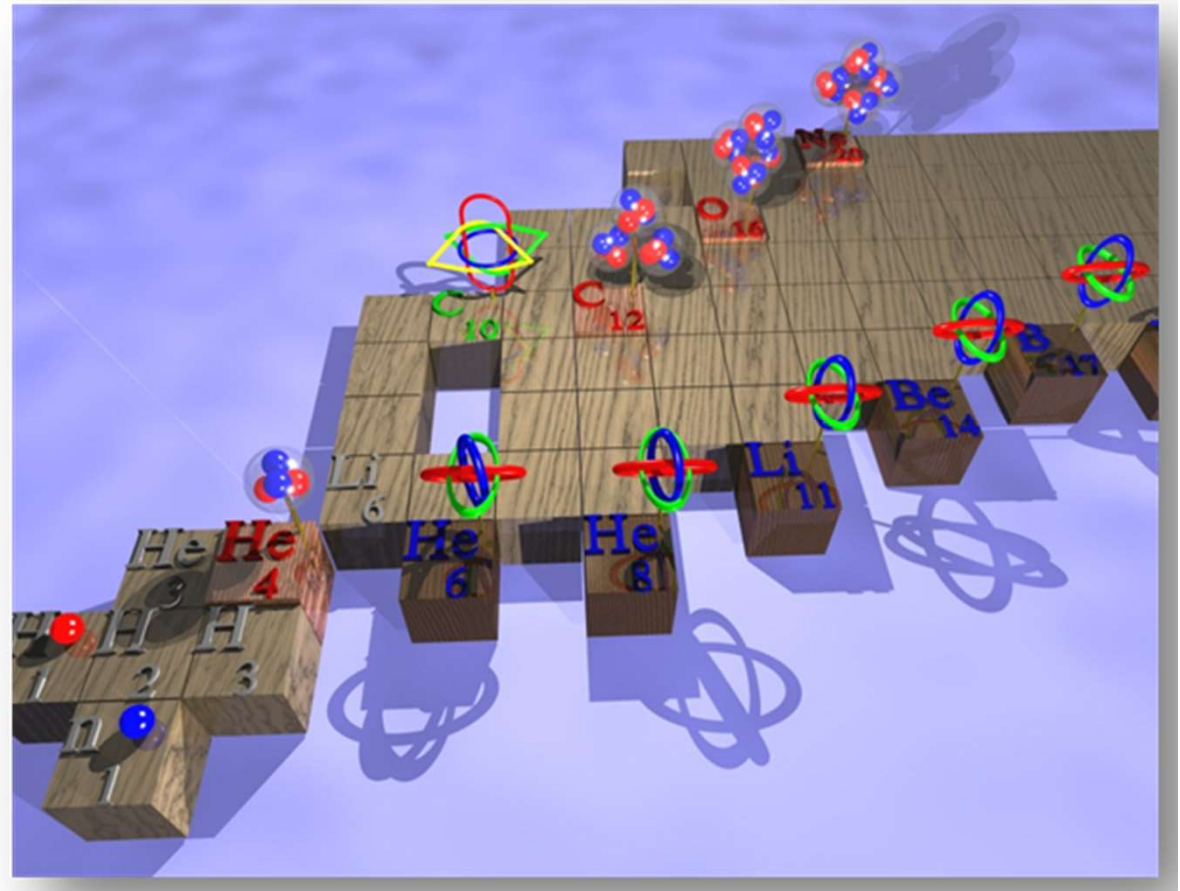
***Laboratoire de Physique Corpusculaire ISMRA and Université de Caen IN2P3-CNRS,  
Caen, France***

F. Haas

***Université de Strasbourg, IN2P3-CNRS Institute Pluridisciplinaire Hubert Curien,  
Strasbourg, France***

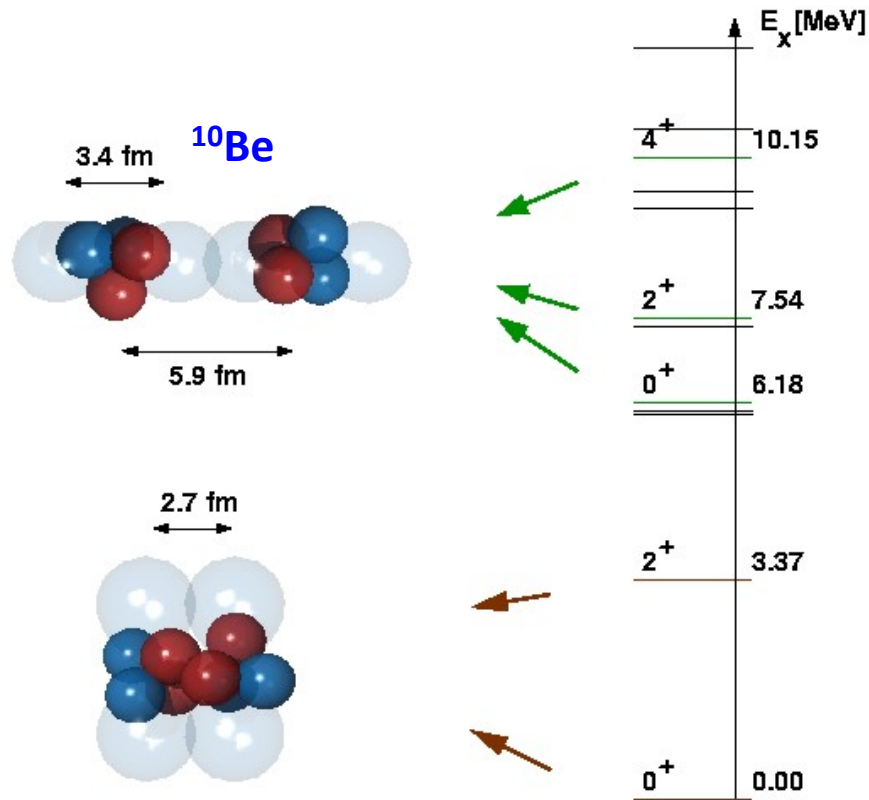
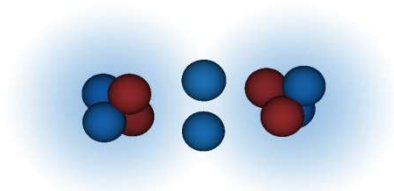
# Advantages of light nuclei

- small number of degrees of freedom
- low density of states at moderate excitations
- tests of basic principles of nuclear structure and interaction starting from individual nucleons and interaction between them
- structure & reactions: single particle – correlated pairs – clusters
- experimentally found p and n drip lines
- richness of unusual nuclear configurations: clusters, Borromean (3 and 4 component systems), skin, halo, molecules

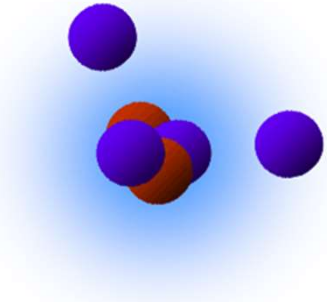
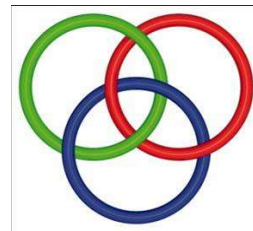


# Nuclear molecules

valence neutrons exchanged between the cores  
 $9,10,12\text{Be}$ ,  $14,16\text{C}$ ,  $18,20,22\text{O}$



Decay by  ${}^6\text{He}$  emission:  ${}^{10,12}\text{Be}$   
 signature of exotic structure -  
 molecular structure



N.Soić *et al*,  
 Europhys.Lett. (1995)

M.Milin *et al*,  
 Europhys.Lett. (1999)

M.Milin *et al*,  
 Nucl.Phys. (2005)

M.Freer *et al*,  
 Phys.Rev.Lett. (2006)

Borromean system  
 neutron halo

# Oxygen isotopes

$^{16}\text{O}$ : double magic ground state, 1<sup>st</sup> excited state  $^{12}\text{C}+\alpha$  cluster structure, possible  $4\alpha$  cluster structure at high excitations

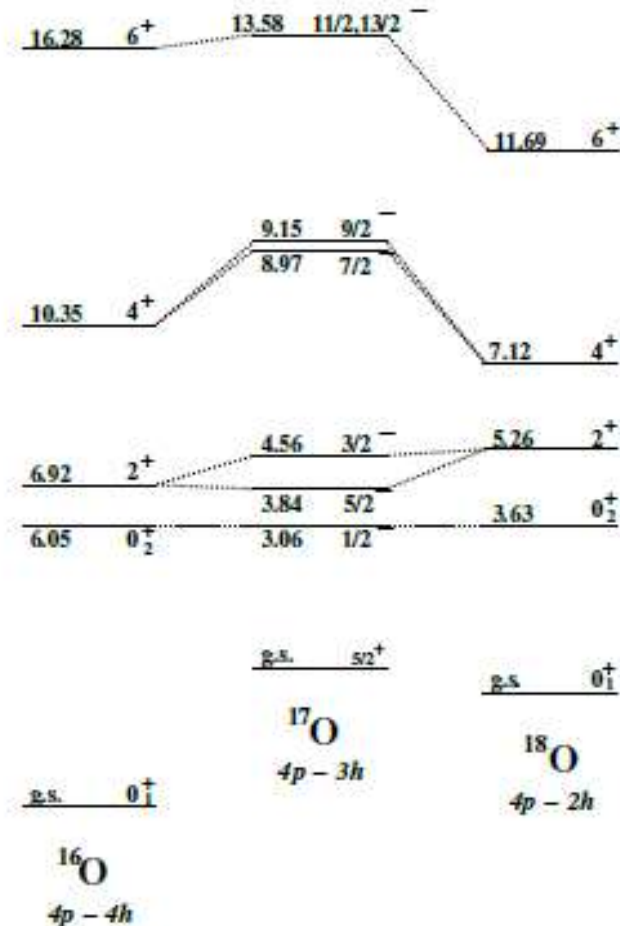
$K^\pi = 0^+$  rotational band

$J^\pi$	$E_x$ MeV
$0^+$	6.05
$2^+$	6.92
$4^+$	10.36
$6^+$	16.28

$K^\pi = 0^-$  rotational band

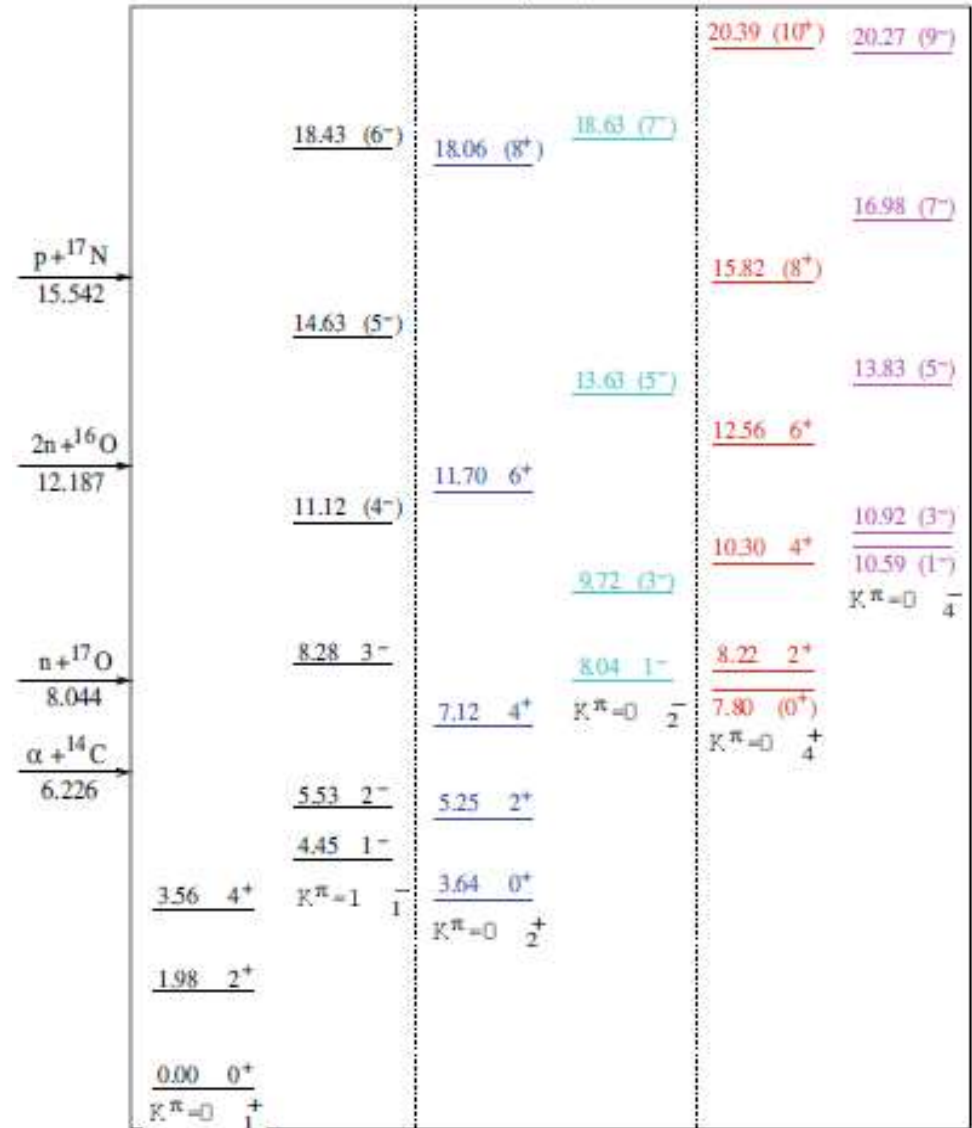
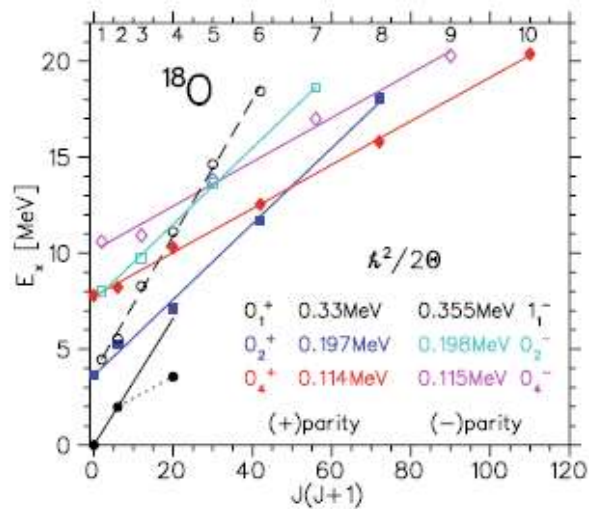
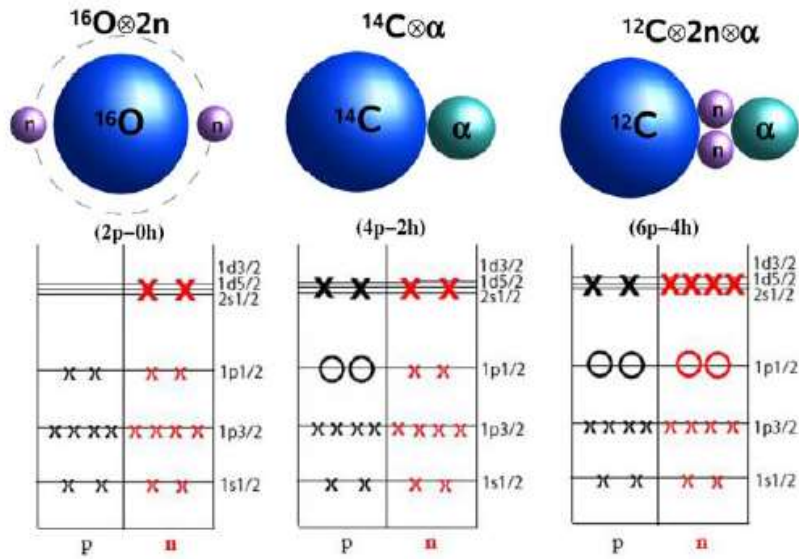
$J^\pi$	$E_x$ MeV
$1^-$	9.59
$3^-$	11.60
$5^-$	14.66
$7^-$	20.86

Plot of the  $4p$ - $nh$  states for the  $^{16-18}\text{O}$



# $^{18}\text{O}$ proposed cluster configurations

W. von Oertzen et al, Eur. Phys. J. A 43 (2010) 17

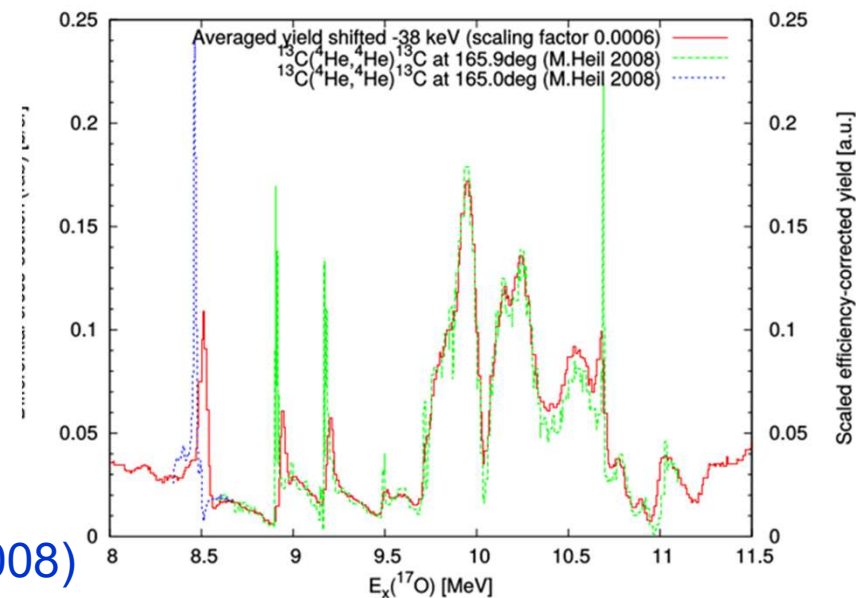
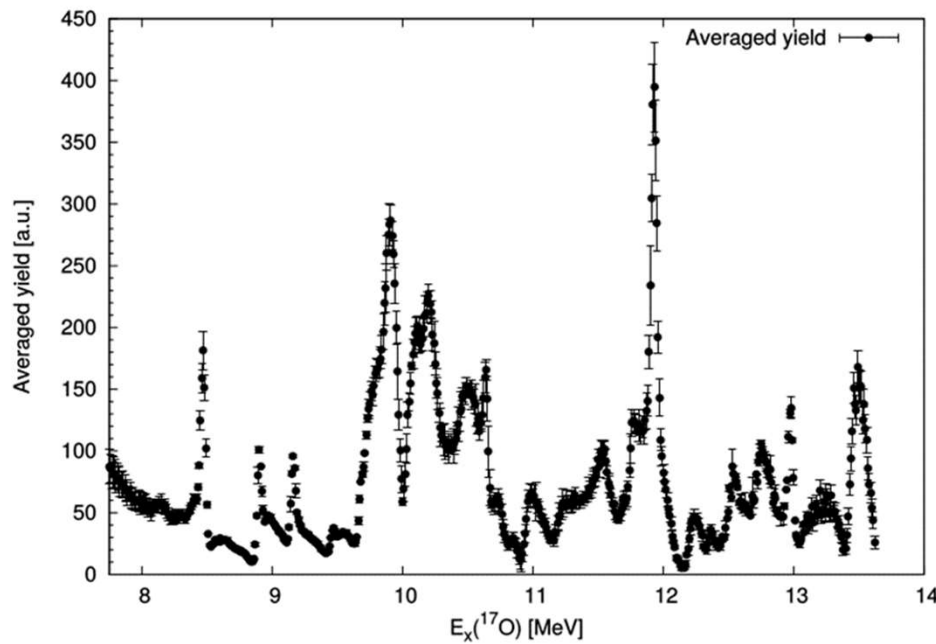
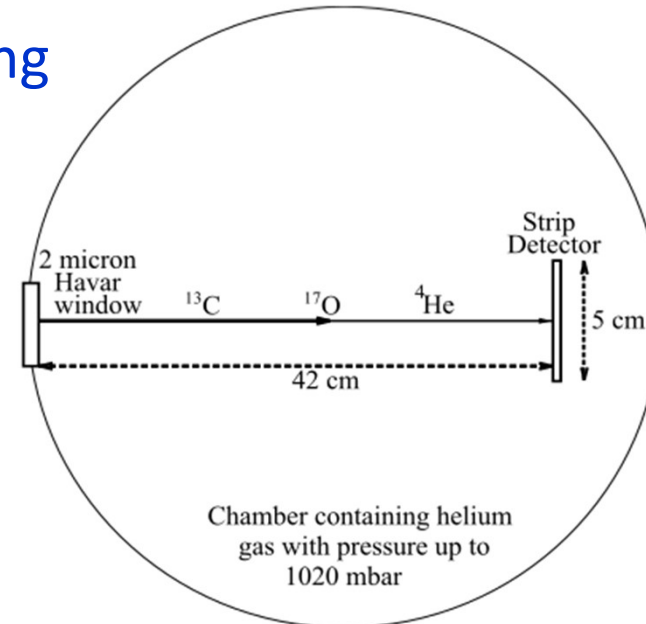




# Experiment: Tandem RBI Zagreb Croatia

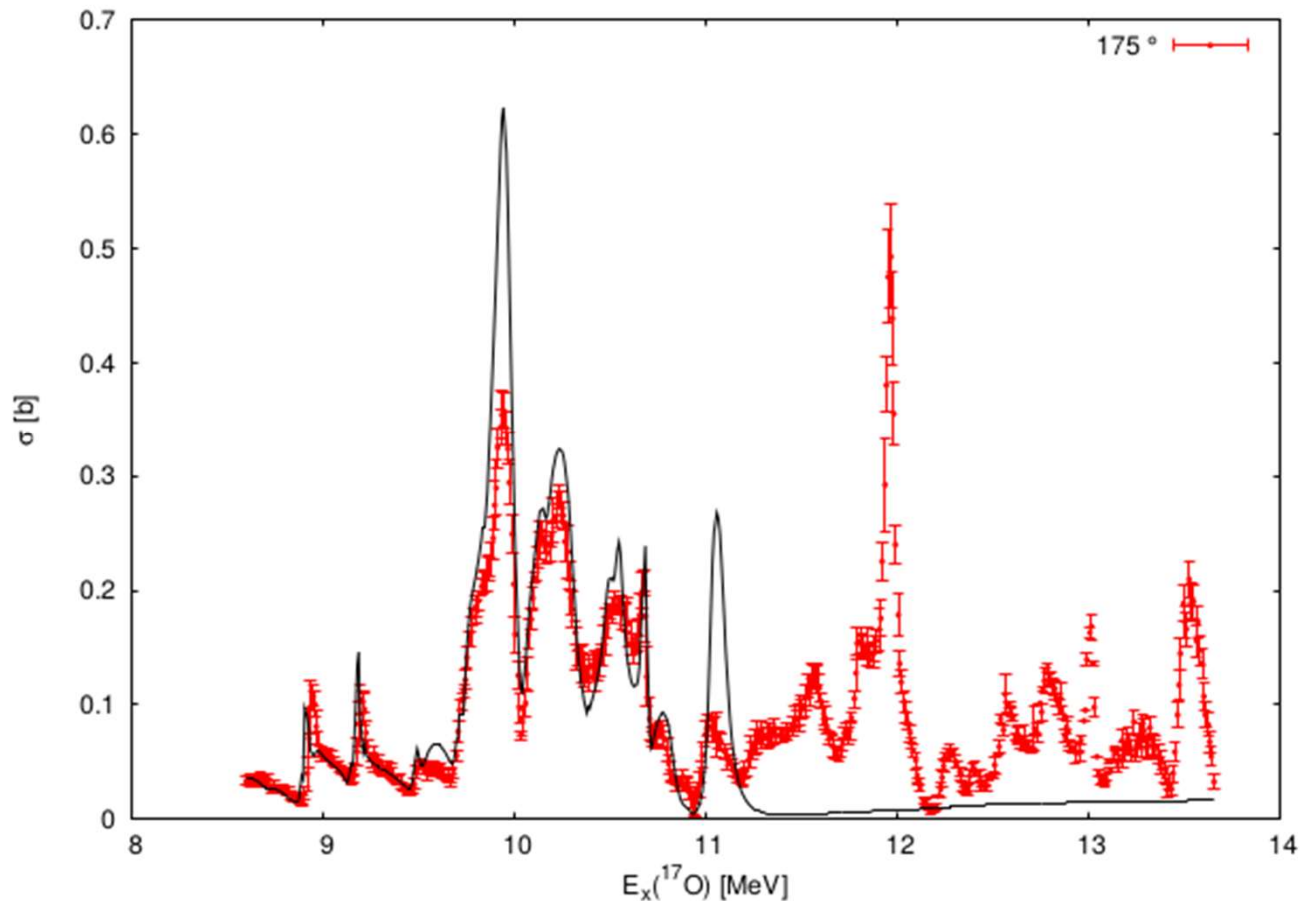
## $^{13}\text{C}+^4\text{He}$ thick gas target resonant scattering

$E_{^{13}\text{C}}$ [MeV]	$p_{^4\text{He}}$ [mbar]	Inelastic-free $E_x(^{17}\text{O})$ range	Run numbers
20.00	312	7.977 – 11.066	25
25.00	461	9.154 – 12.243	27
30.00	591, 589, 587	10.331 – 13.420	28-30, 32
33.00	699	11.037 – 14.126	33
35.00	720	11.508 – 14.597	35



Published data: M Heil et al, PRC 78 (2008) 025803, up to excitation of 11.5 MeV

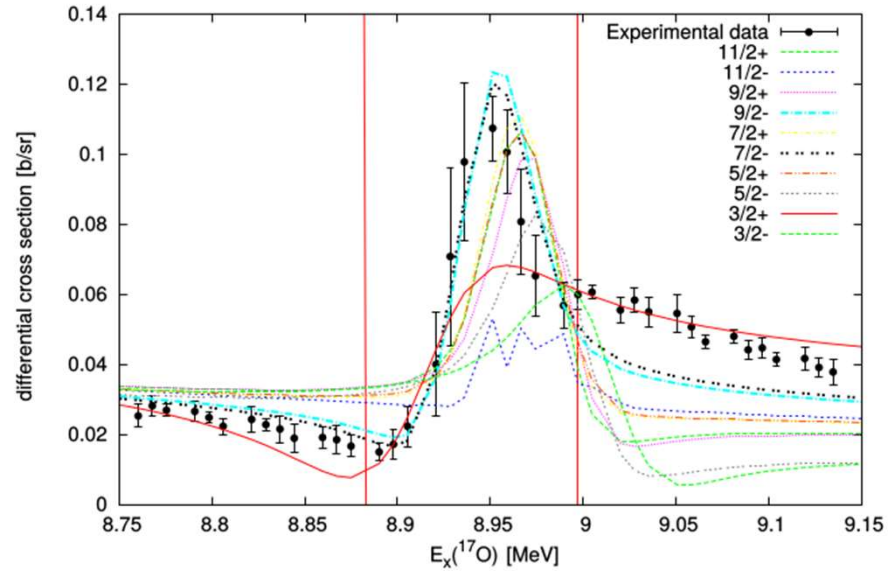
- R-matrix fits using code AZURE2 with resonance parameters from M. Heil et al (70 resonances at excitations 4.55 – 15.44 MeV obtained using code SAMMY)
- extensive fits of all available data for the  $^{13}\text{C}+^4\text{He}$  elastic scattering at the number of angles, elastic and inelastic (1st and 2nd excited state)  $^{16}\text{O}+n$  scattering,  $^{13}\text{C}(^4\text{He},n)$  reaction,  $^{16}\text{O}(n,^4\text{He})$  reaction
- significant discrepancies between fits and experimental results even for Heil data



Our results for the  $^{13}\text{C}+^4\text{He}$  elastic scattering with R-matrix fit using published resonance parameters

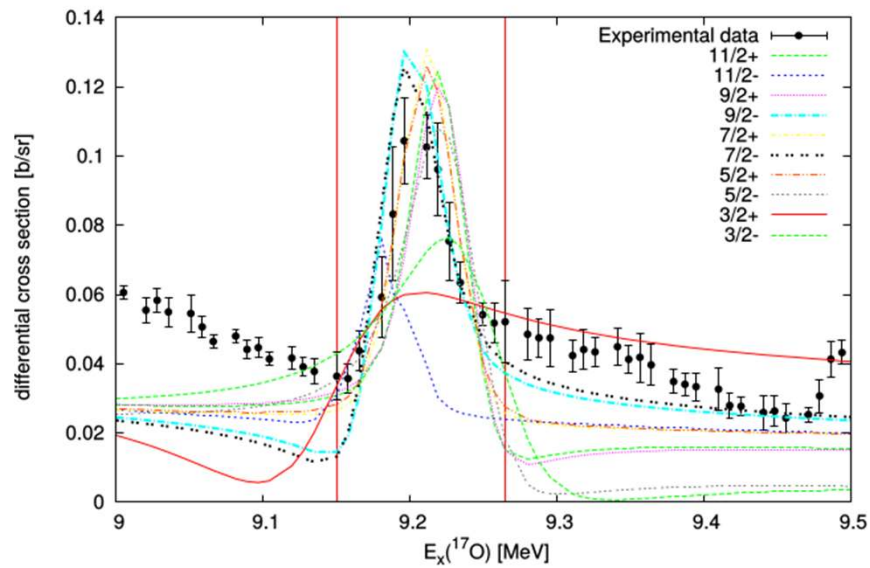


# Simplified R-matrix fit: single isolated resonance for single channel and single data set at one angle



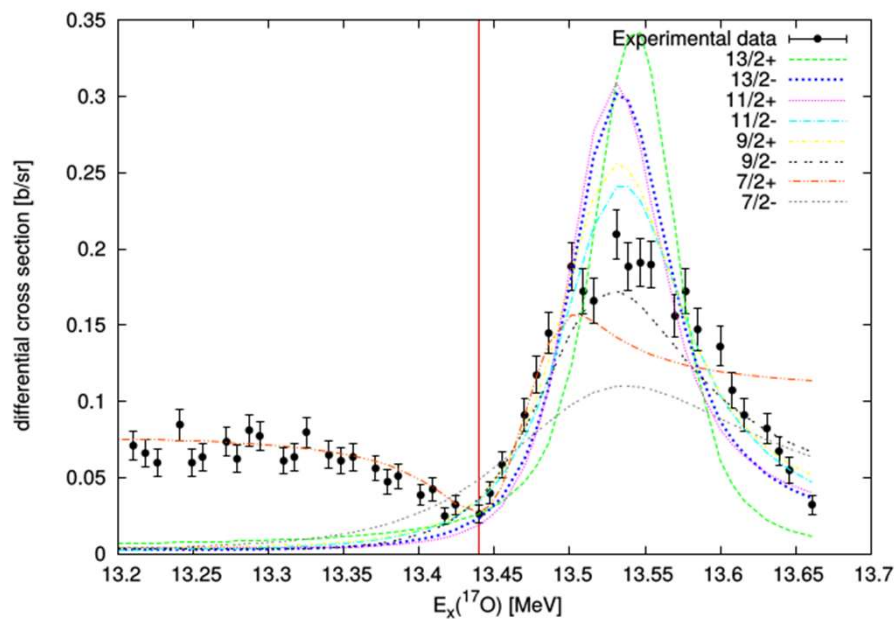
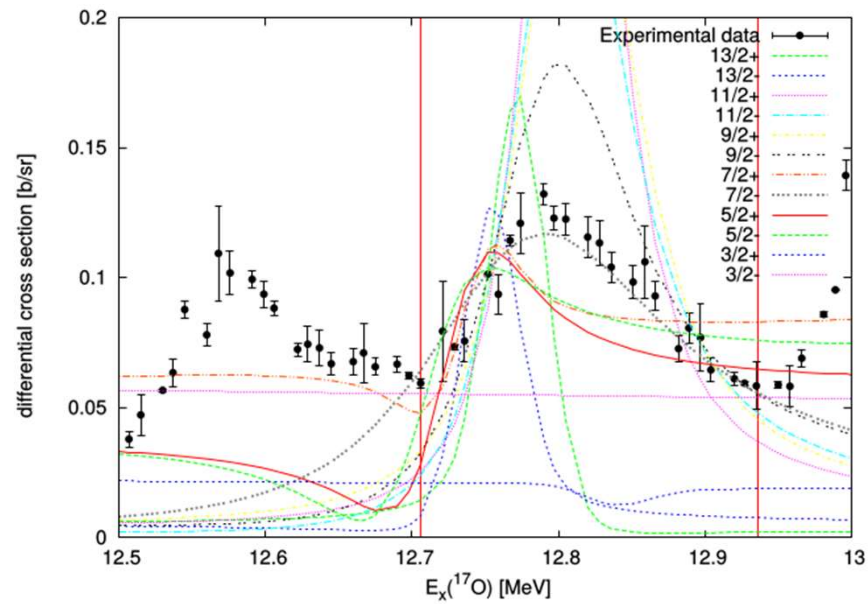
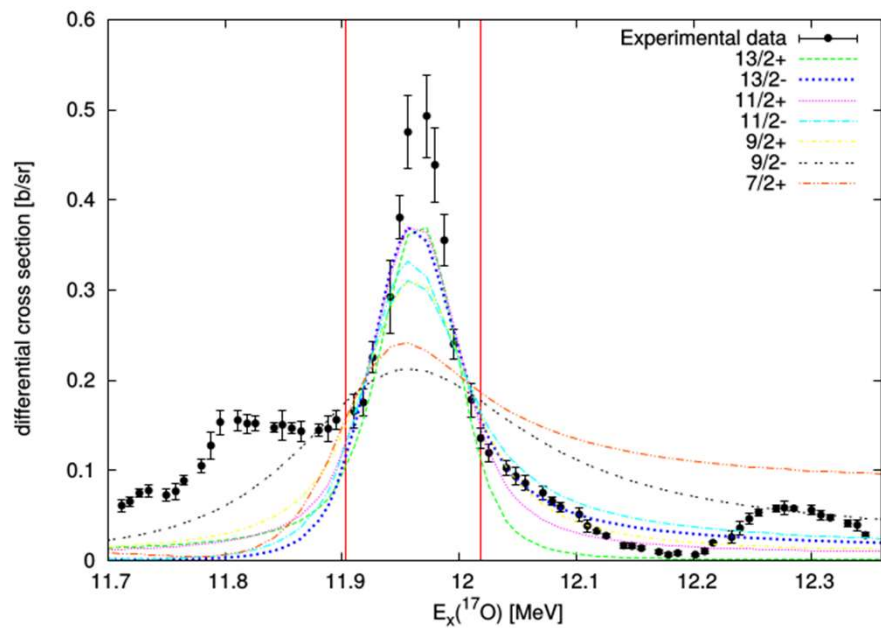
## Test fits

$J^\pi$	Peak			
	8.9 MeV		9.2 MeV	
	$\gamma$ [MeV <sup>1/2</sup> ]	$\theta_W^2$	$\gamma$ [MeV <sup>1/2</sup> ]	$\theta_W^2$
$\frac{9}{2}^-$	-0.482501	0.307	0.408232	0.220
$\frac{7}{2}^-$	-0.632510	0.528	0.538238	0.382



## Heil et al results

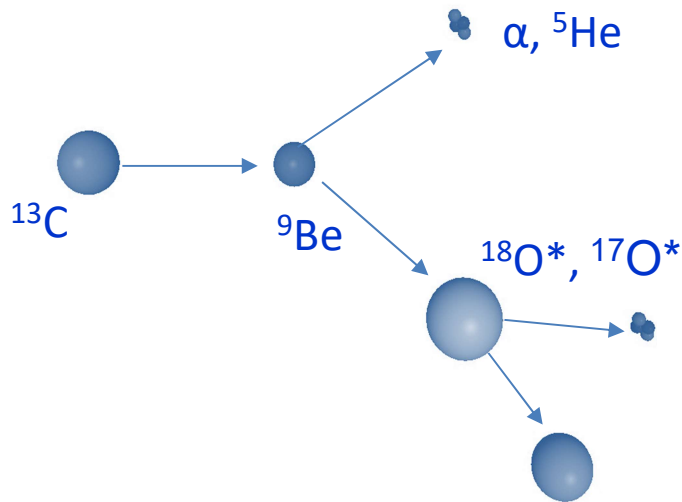
$J^\pi$	$E_x(^{17}\text{O})$ [MeV]	$\Gamma_n$ [keV]	$\Gamma_\alpha$ [keV]
$\frac{9}{2}^-$	8.9029	$-2.3 \cdot 10^{-5}$	-0.45
$\frac{7}{2}^-$	9.1737	0.038	3.26



Peak								
12.0 MeV			12.8 MeV			13.6 MeV		
$J^\pi$	$\gamma$ [MeV <sup>1/2</sup> ]	$\theta_W^2$	$J^\pi$	$\gamma$ [MeV <sup>1/2</sup> ]	$\theta_W^2$	$J^\pi$	$\gamma$ [MeV <sup>1/2</sup> ]	$\theta_W^2$
$\frac{11}{2}^+$	0.339962	0.153	$\frac{7}{2}^-$	0.284347	0.107	$\frac{11}{2}^-$	0.431423	0.246
$\frac{13}{2}^-$	0.837051	0.925						

# Experiment: Tandem IPN Orsay France

Kinematically complete measurements - detected 2 of 3 reaction products

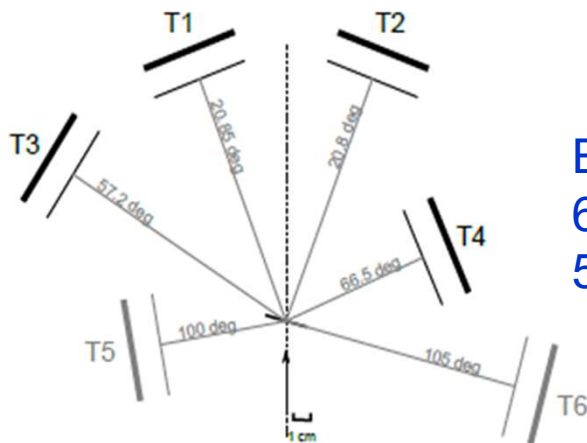


$$E_{\text{thr}}(\alpha + ^{13}\text{C}) = 6.361 \text{ MeV}$$



$$E_{\text{thr}}(\alpha + ^{14}\text{C}) = 6.228 \text{ MeV}$$

$$E_{\text{thr}}(^6\text{He} + ^{12}\text{C}) = 18.380 \text{ MeV}$$



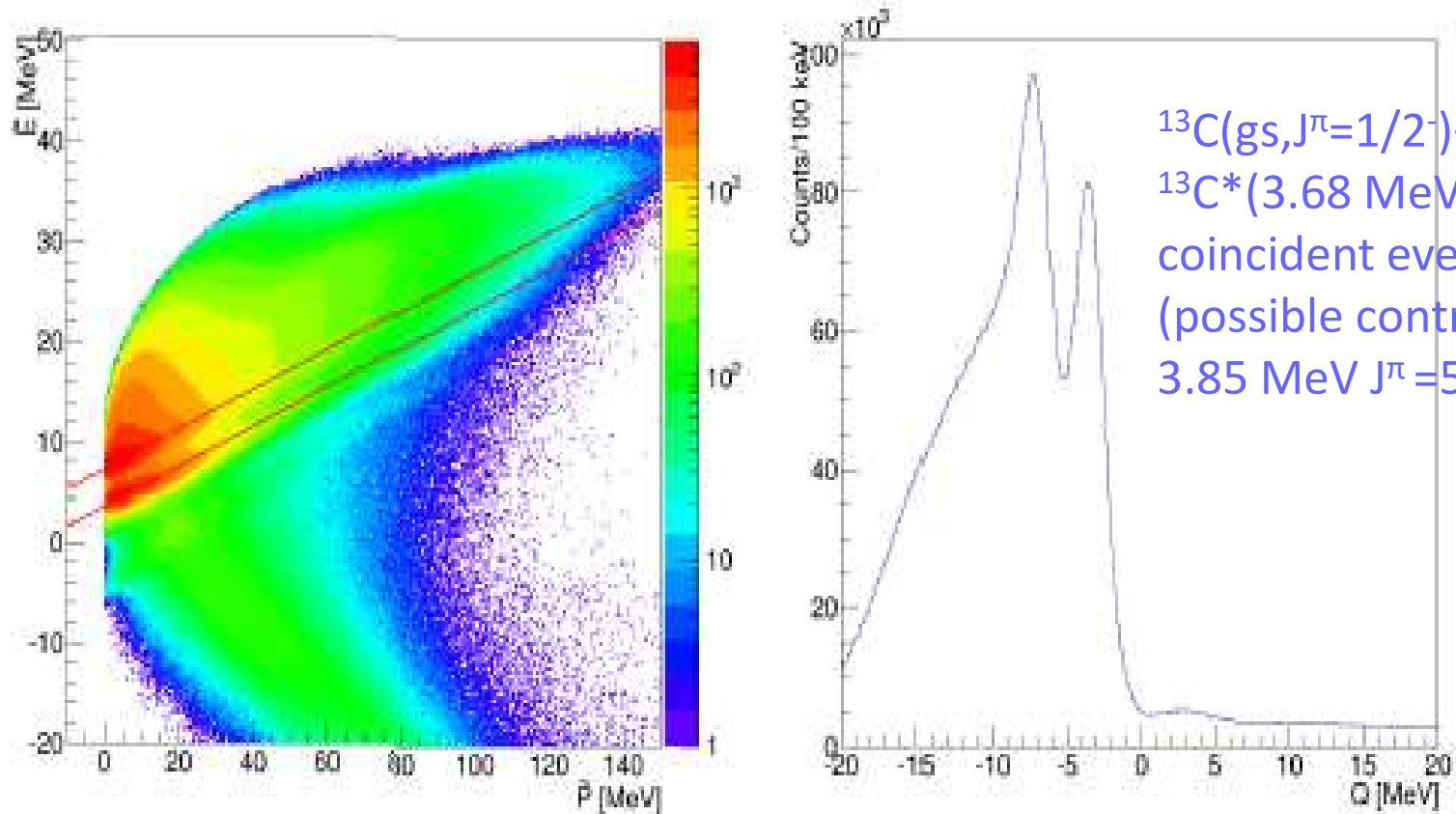
$E(^{13}\text{C})_{\text{beam}} = 72 \text{ MeV}$ ,  $^9\text{Be}$  target thickness  $100 \mu\text{g}/\text{cm}^2$   
 6 telescopes  $20 \mu\text{m}$  SSSD +  $1000 \text{ DSSSD } \mu\text{m}$ ,  
 $50 \times 50 \text{ mm}^2$  Micron Semiconductor type W1

Goal: characterization of the  $^{17,18}\text{O}$  resonances decaying by helium emission in excitation energy range 7 - 25 MeV: excitation energy, widths

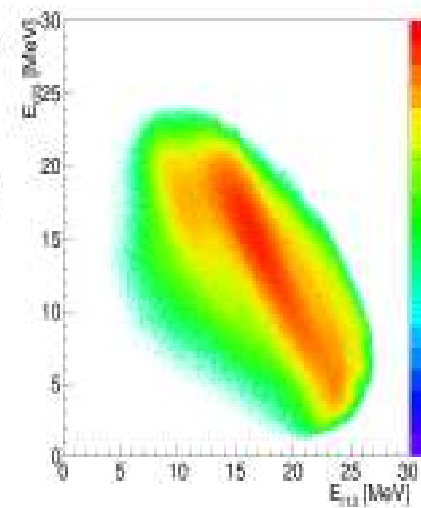
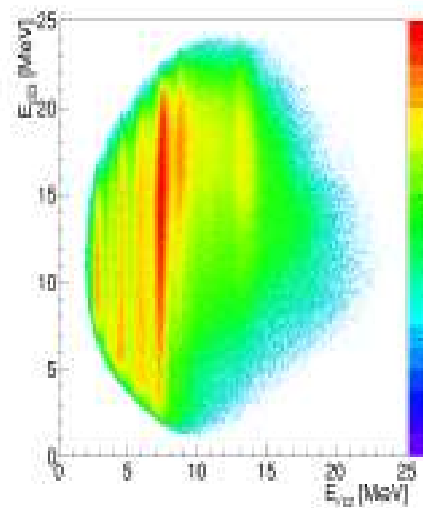
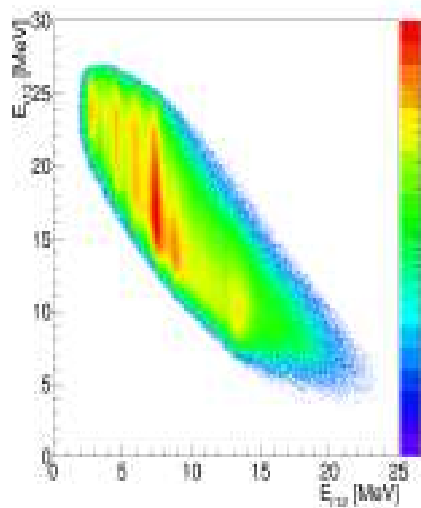
# $^{17}\text{O}$ results



$^{13}\text{C}(\text{T1})$ - $^4\text{He}(\text{T2})$ ,  $^{13}\text{C}(\text{T2})$ - $^4\text{He}(\text{T1})$ ,  $^{13}\text{C}(\text{T1})$ - $^4\text{He}(\text{T4})$  &  $^{13}\text{C}(\text{T2})$ - $^4\text{He}(\text{T3})$  coincident events



Reaction identification: Catania plot & Q-value plot

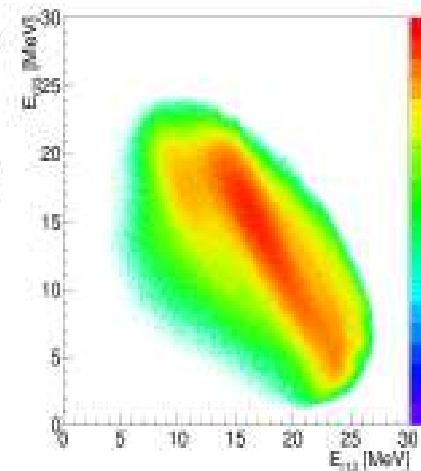
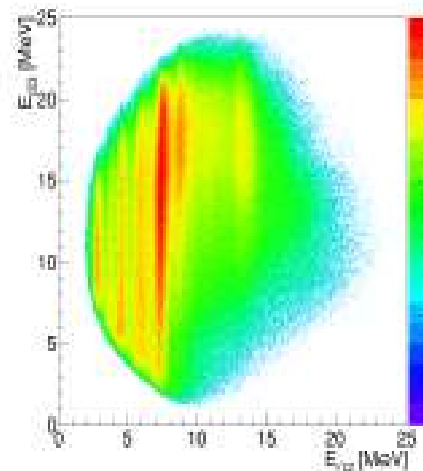
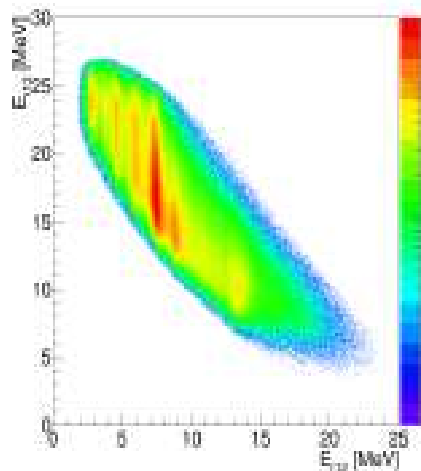


Exit channel  
 $^{13}\text{C}+^4\text{He}+^5\text{He}$

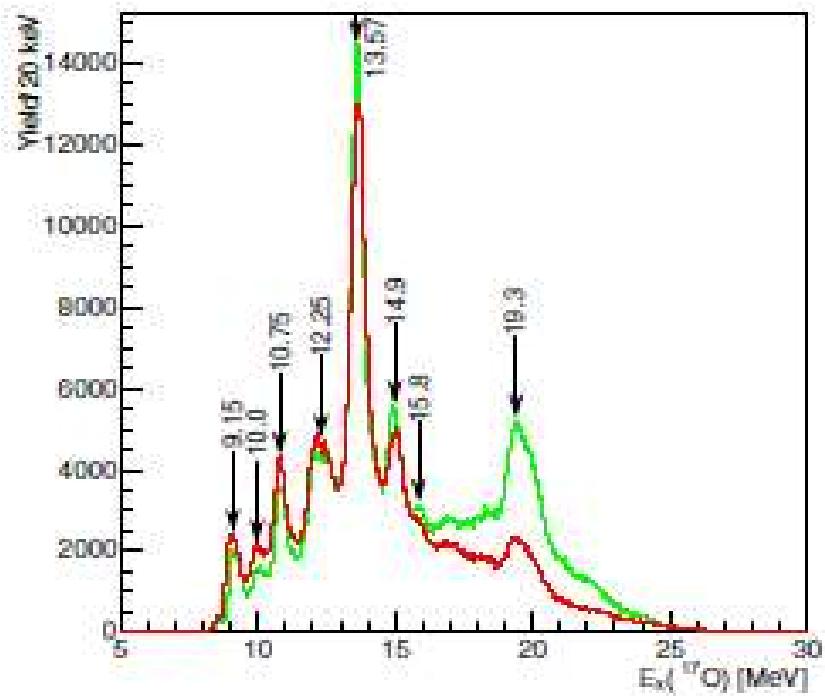
$^{17}\text{O} = ^{13}\text{C}+^4\text{He}$   
 T1-T2 events

$^9\text{Be} = ^4\text{He}+^5\text{He}$   
 T1-T4, T2-T3  
 events

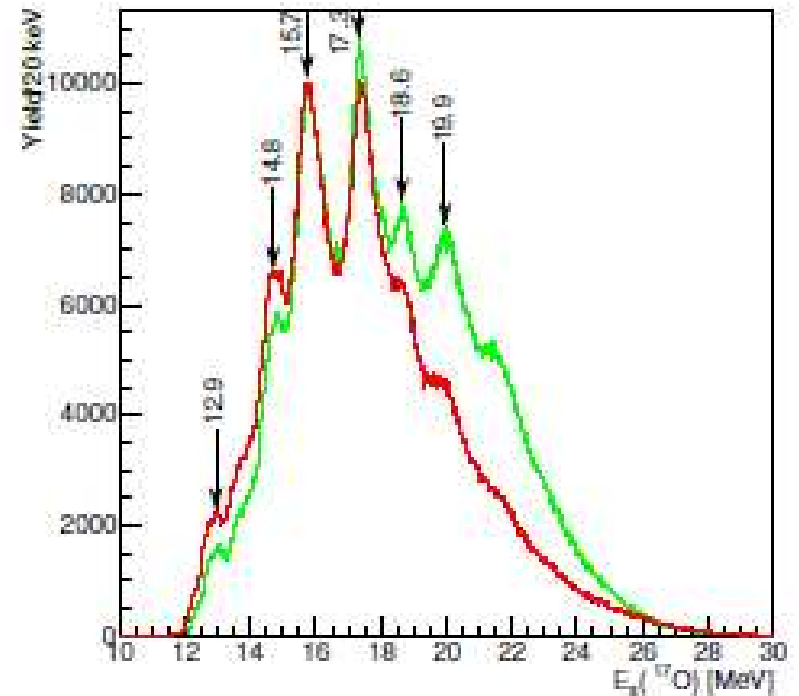
$^{18}\text{O} = ^{13}\text{C}+^5\text{He}$   
 not observed



Relative-energy plots for the  $^9\text{Be}(^{13}\text{C}, ^{13}\text{C}^4\text{He})^5\text{He}$  reaction. The  $^{13}\text{C}$ (T1/T2),  $^4\text{He}$ (T2/T1) and  $^5\text{He}$  (undetected) are labeled by numbers 1, 2 and 3.



The  $^{17}\text{O}$  excitation energy spectrum from the  $^{13}\text{C}(\text{gs}, J^\pi=1/2^-)+^4\text{He}$  coincident events in T1-T2 (red) and T2-T1 (green).



The  $^{17}\text{O}$  excitation energy spectrum from the  $^{13}\text{C}^*(3.68 \text{ MeV}, J^\pi = 3/2^-)+^4\text{He}$  coincident events in T1-T2 (red) and T2-T1 (green) (possible contribution 3.85 MeV  $J^\pi=5/2^+$ )



No.	$^{13}\text{C}+^4\text{He}$ res. el.		$^{13}\text{C}+^9\text{Be}$ reactions		References	Tilley <i>et al.</i> [50]	
	$E_x$ [MeV]	$J^\pi$	$^{13}\text{C}+^4\text{He}$ coinc.	$^{13}\text{C}^*+^4\text{He}$ coinc.		$E_x$ [MeV]	$J^\pi$
1	8.9	$\left(\frac{7^-}{2}\right)$ or $\left(\frac{9^-}{2}\right)$			[7]		
2	9.2	$\left(\frac{7^-}{2}\right)$ or $\left(\frac{9^-}{2}\right)$	9.15		[5], [7], [98], [101], [102]	9.147	$\frac{1^-}{2}$
3	10.0 <sup>†</sup>		10.0		[7]	9.976	$\frac{5^-}{2}$
4	10.75 <sup>†</sup>		10.75		[6], [100], [101]	10.777	$\frac{1^+}{2}, \frac{7^-}{2}$
5	12.0	$\left(\frac{11^+}{2}\right)$ or $\left(\frac{13^-}{2}\right)$	12.25 (wide)		[61], [96], [97], [98]	12.005 ± 15	$> \frac{3}{2}$
6	12.8			12.9		[100]	12.93
7	13.6	$\left(\frac{11^-}{2}\right)$	13.57		[4], [5], [98], [100]	13.58	$\left(\frac{11}{2}, \frac{13}{2}\right)^-$
8			14.9	14.8	[4], [6], [100]	15.1 ± 0.1	$\left(\frac{9^+}{2}, \frac{11^+}{2}\right)$
9			15.8	15.7	[4], [6]*, [100], [103],	15.95	$\left(\frac{9^+}{2}, \frac{11^+}{2}\right)$
10			(weak peak)	17.3	[3], [6]*, [98], [105]	17.06	$\frac{11^-}{2}$
11			(weak peak)	18.6	[6]*	18.72	
12			19.3		[6], [4], [104]		
13				19.6		[3], [6]*	19.6

Published results:

(6) M. Milin et al, EPJ A 41 (2009) 335, the same reaction

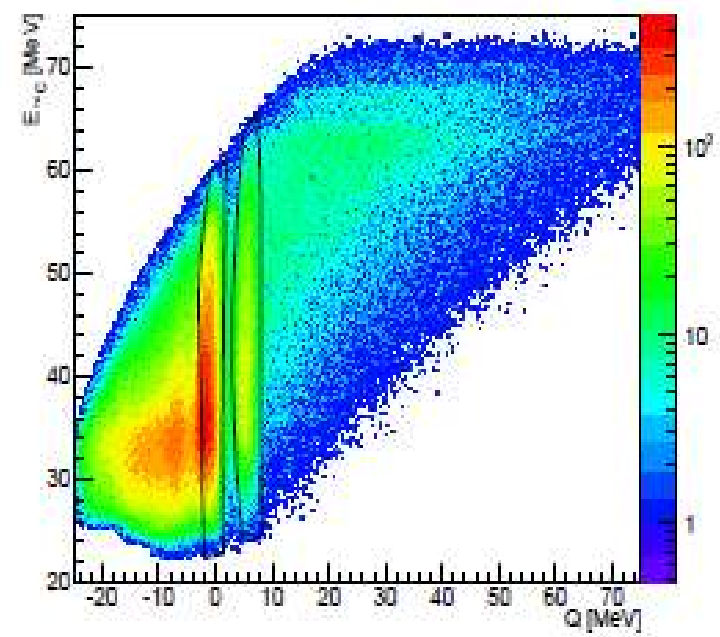
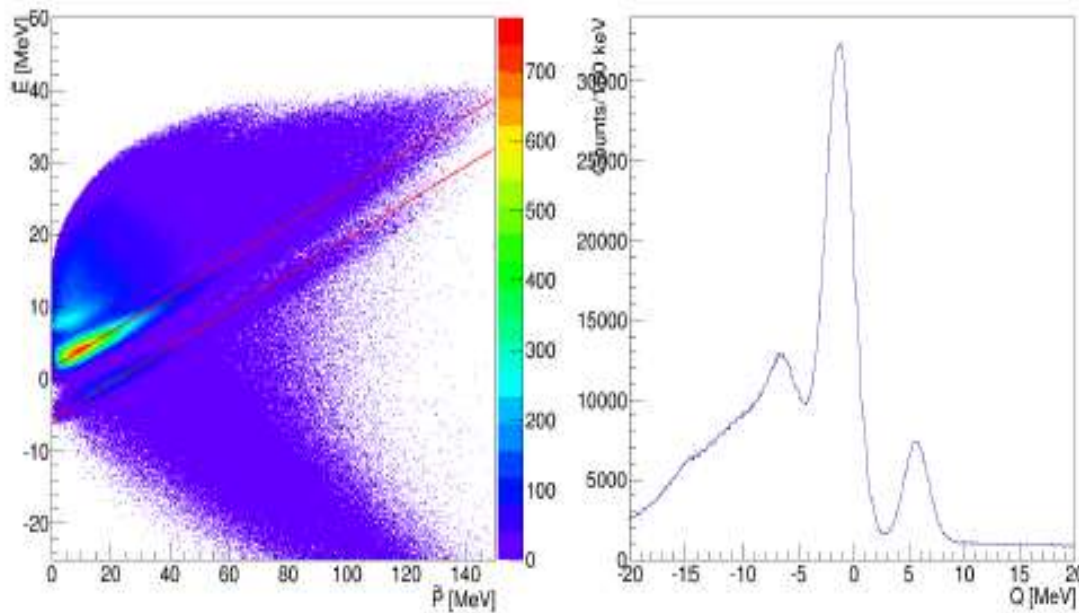
(7) M. Heil et al, PRC 78 (2008) 025803, the  $^{13}\text{C}+^4\text{He}$  thick target resonant scattering up to excitation 11.1 MeV

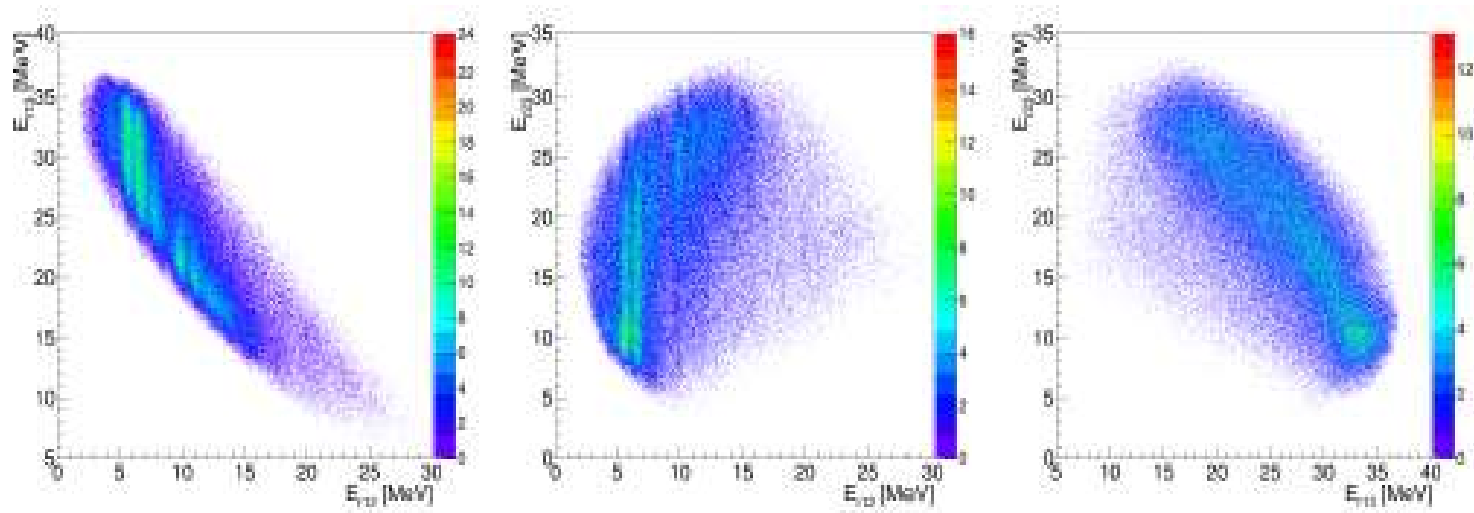
# $^{18}\text{O}$ results



Events for all possible telescope combinations

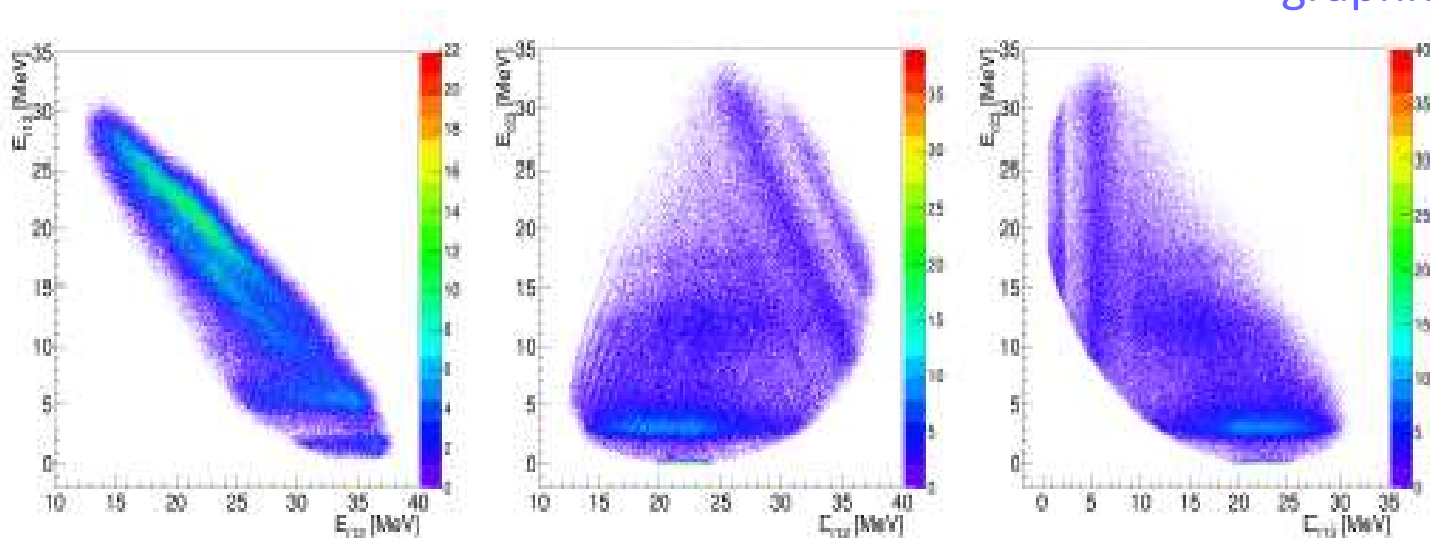
$^{14}\text{C}(\text{T1}) - ^4\text{He}(\text{T2})$      $^{14}\text{C}(\text{gs}, J^\pi = 0^+) + ^4\text{He}$  &  $^{14}\text{C}^*(7 \text{ MeV}) + ^4\text{He}$  in T1-T2



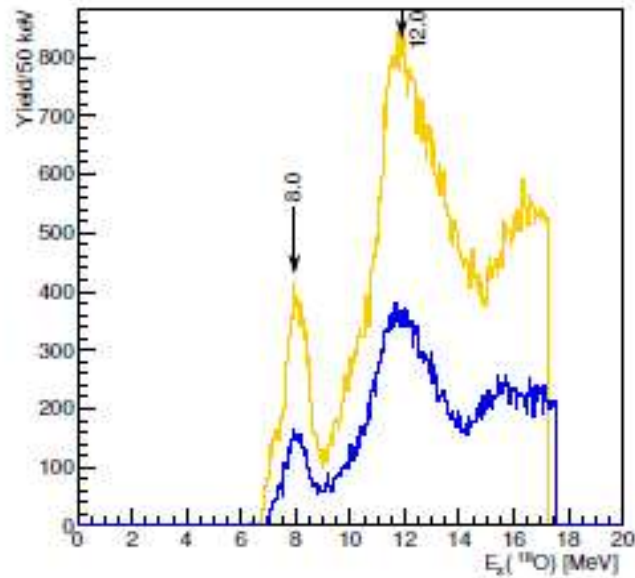
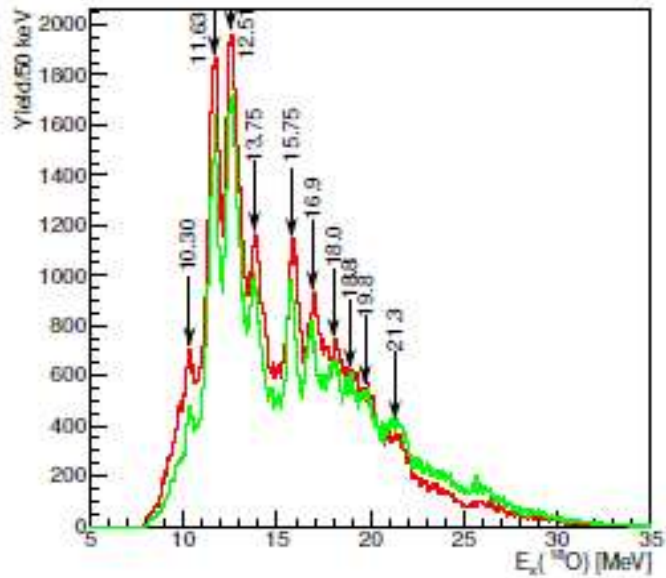


Relative-energy plots for the  ${}^9\text{Be}({}^{13}\text{C}, {}^{14}\text{C}){}^4\text{He}$  reaction. The  ${}^{14}\text{C}(\text{T1})$ ,  ${}^4\text{He}(\text{T2})$  and  ${}^4\text{He}$  (undetected) are labeled by numbers 1, 2 and 3.

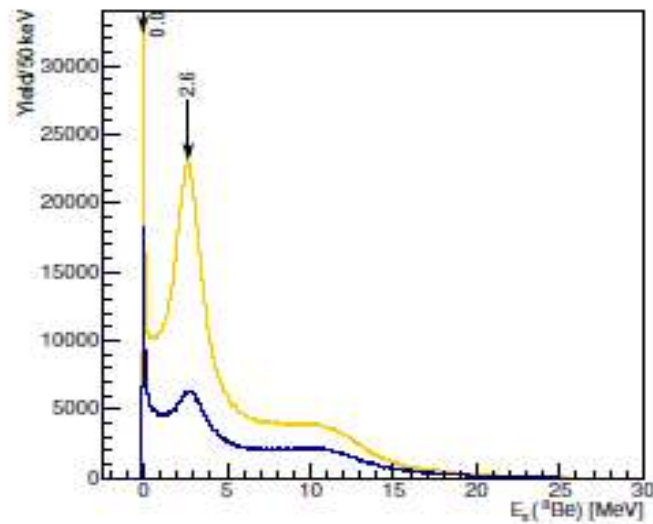
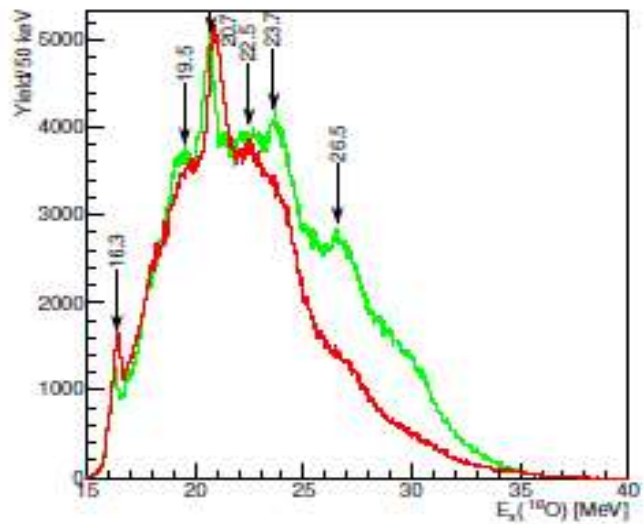
graphical cuts



Relative-energy plots for the  ${}^9\text{Be}({}^{13}\text{C}, {}^{14}\text{C}){}^4\text{He}$  reaction. The  ${}^{14}\text{C}(\text{T1})$ ,  ${}^4\text{He}(\text{T4})$  and  ${}^4\text{He}$  (undetected) are labeled by numbers 1, 2 and 3.

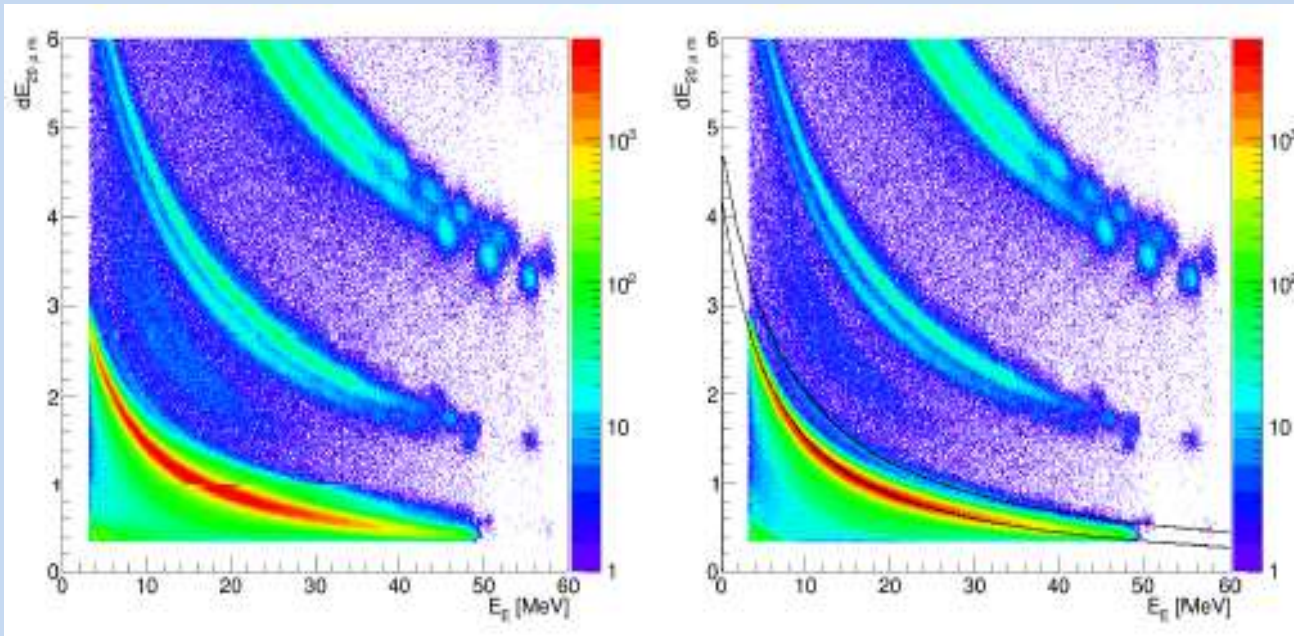


The  $^{18}\text{O}$  excitation energy spectrum for the  $^{14}\text{C}(\text{gs})+^4\text{He}$  coincident events in T1-T2 (red), T2-T1 (green), T1-T4 (orange) and T2-T3 (blue).

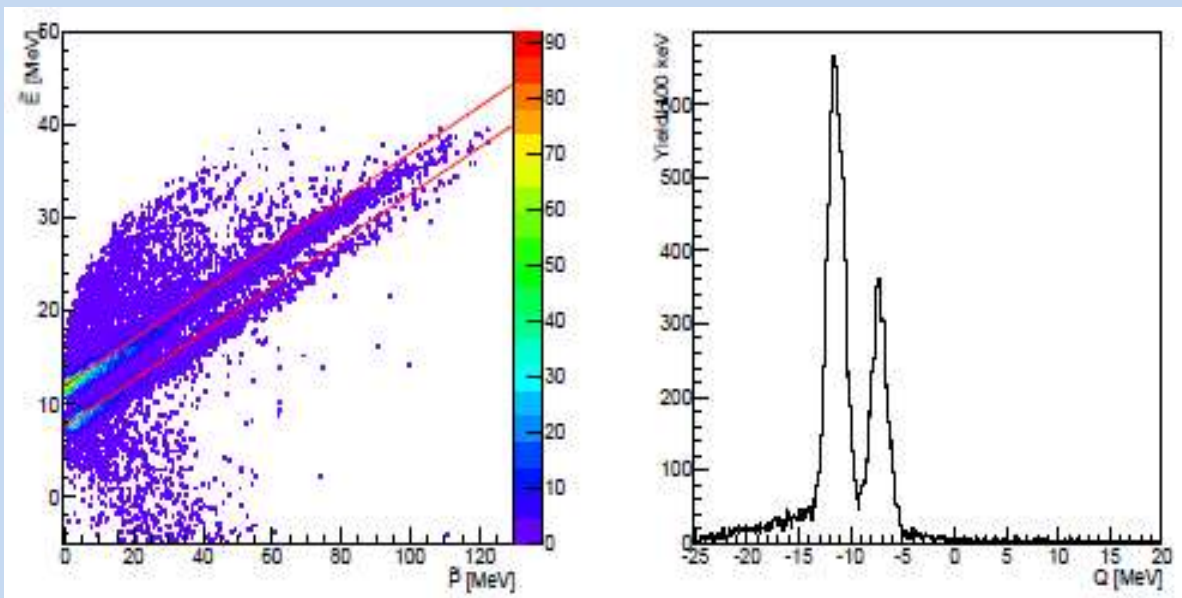


The  $^{18}\text{O}$  excitation energy spectrum for the  $^{14}\text{C}^*(7\text{ MeV})+^4\text{He}$  events in T1-T2 (red) and T2-T1 (green);  $^8\text{Be}$  spectrum for T1-T4 (orange) and T2-T3 (blue).

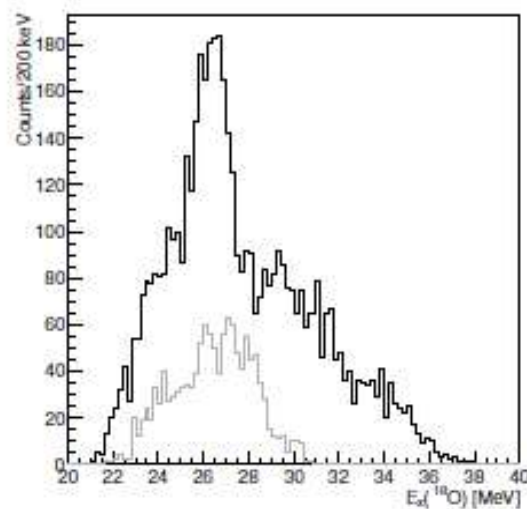
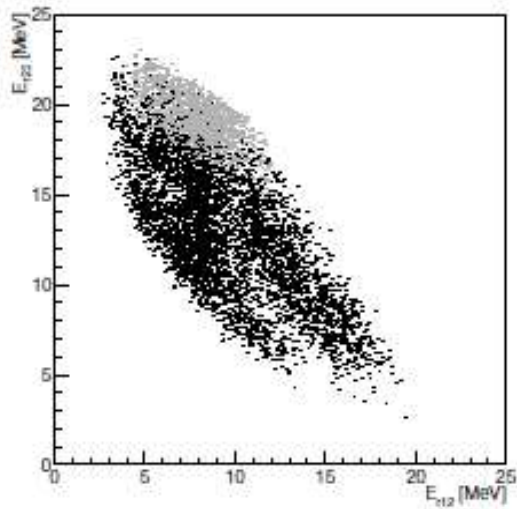
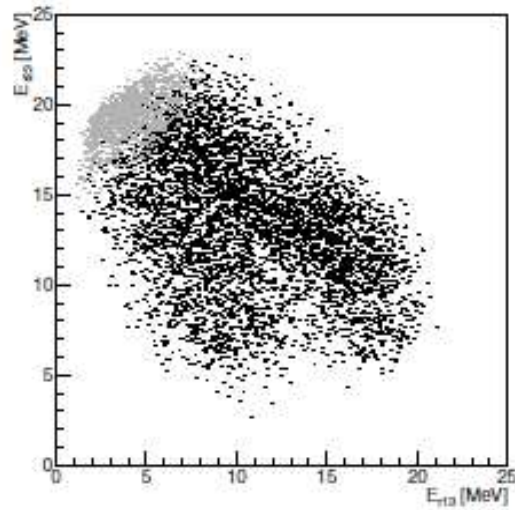
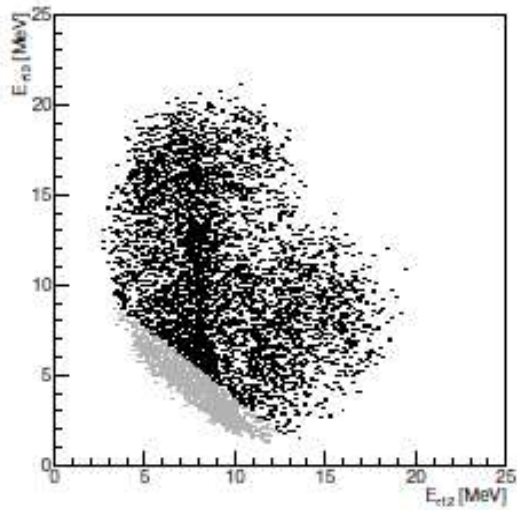




Additional  $\Delta E$ - $E$  spectra filtering to separate  ${}^6\text{He}$  from  ${}^4\text{He}$  for the T1,  $\Delta E$ -strip 8. Black lines show results of simulations for  ${}^4,{}^6\text{He}$  in T1



The Catania plot for the  ${}^6\text{He}$  detected in T1 and  ${}^{12}\text{C}$  in T2. The red lines are predicted loci for the  ${}^9\text{Be}({}^{13}\text{C}, {}^6\text{He}){}^{12}\text{C}(\text{gs}) + {}^4\text{He}$  and  ${}^9\text{Be}({}^{13}\text{C}, {}^6\text{He}){}^{12}\text{C}^*(4.4 \text{ MeV}) + {}^4\text{He}$ .



broad peak at 26.5 MeV,  
indications of peaks at  
29.5 MeV and around  
23.5 MeV.

E-E plots for  ${}^6\text{He}$  and  ${}^{12}\text{C}(\text{gs})$  detected in T1 and T2, labelled as 1 and 2. The last plot is the  ${}^{18}\text{O}$  excitation energy spectrum for events selected via graphical cut (black dots). The grey dots correspond to events from the  ${}^{16}\text{O}$  decay. For the  ${}^{12}\text{C}^*(4.4 \text{ MeV})+{}^6\text{He}$  events excitation spectrum is structureless.

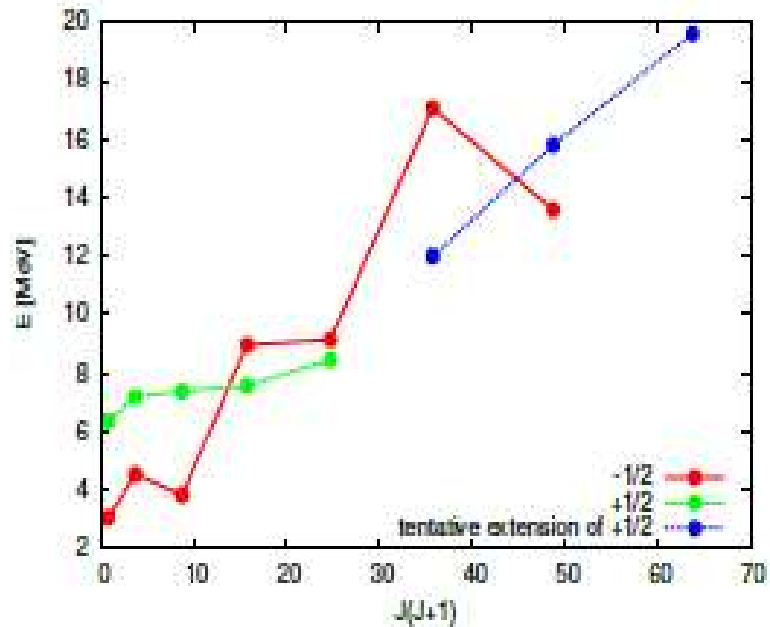


No. 1	$E_x(^{18}\text{O})$ from the $^{13}\text{C}+^9\text{Be}$ reactions			References	Tilley <i>et. al.</i> [87]	
	$^{14}\text{C}+^4\text{He}$	$^{14}\text{C}^*+^4\text{He}$	$^{12}\text{C}+^6\text{He}$		$E_x$ [MeV]	$J^\pi$
2	10.30 MeV			[12], [13], [14], [106], [107], [108], [109], [110], [111], [112], [113], [114]	10.290 MeV	$4^+$
3	11.63 MeV			[12], [13], [14], [101], [106], [107], [108], [109], [111], [113]	11.62 MeV	$5^-$
4	12.51 MeV			[12], [13], [14], [106], [107], [108], [109], [111]	12.53 MeV	$6^+$
5	13.75 MeV			[111]	13.8	$1^-$
6				[13], [14]	13.82	$5^-$
7	15.75 MeV			[111]	15.8	$1^-$
8		16.1 MeV		[12]	16.315	$(3,2)^-$
9	16.9 MeV			[107], [109]	16.948	$(2,3)^-$
10	18.0 MeV			[115]	18.049	
11	18.8 MeV			[110], [115]	18.68	$(4^-)$
12		19.3 MeV				
13	19.8 MeV					
14		20.5 MeV		[110]	20.86	
15	21.3 MeV			[110], [117]	21.42	$(4^-)$
16		22.3 MeV		[110]	22.4	$4^-$
17		23.5 MeV	23.5 MeV	[110], [116]	23.8	$1^-$
18		26.3 MeV	26.5 MeV	[116]	27	$1^-$
19			29.5 MeV	[116]	30	

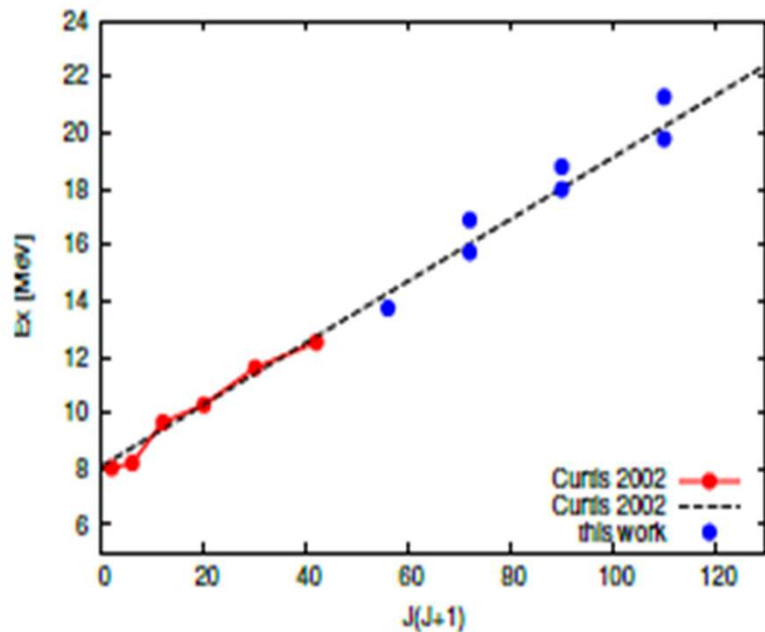
Published many results, some recent:

(14) M. L. Avila et al, PRC 90 (2014) 024327, the  $^{14}\text{C}+^4\text{He}$  thick target resonant scattering

(12) N. Curtis et al, PRC 66 (2002) 024315,  $^{14}\text{C}(^{18}\text{O}, ^{14}\text{C}^4\text{He})^{14}\text{C}$



A tentative extension of the proposed  $^{17}\text{O}$  positive-parity rotational band and the negative-parity rotational band.



A tentative extension of the proposed  $^{18}\text{O}$  rotational band. In agreement with proposed rotational bands in W. von Oertzen et al, EPJ A 43 (2009) 17

## Summary & outlook

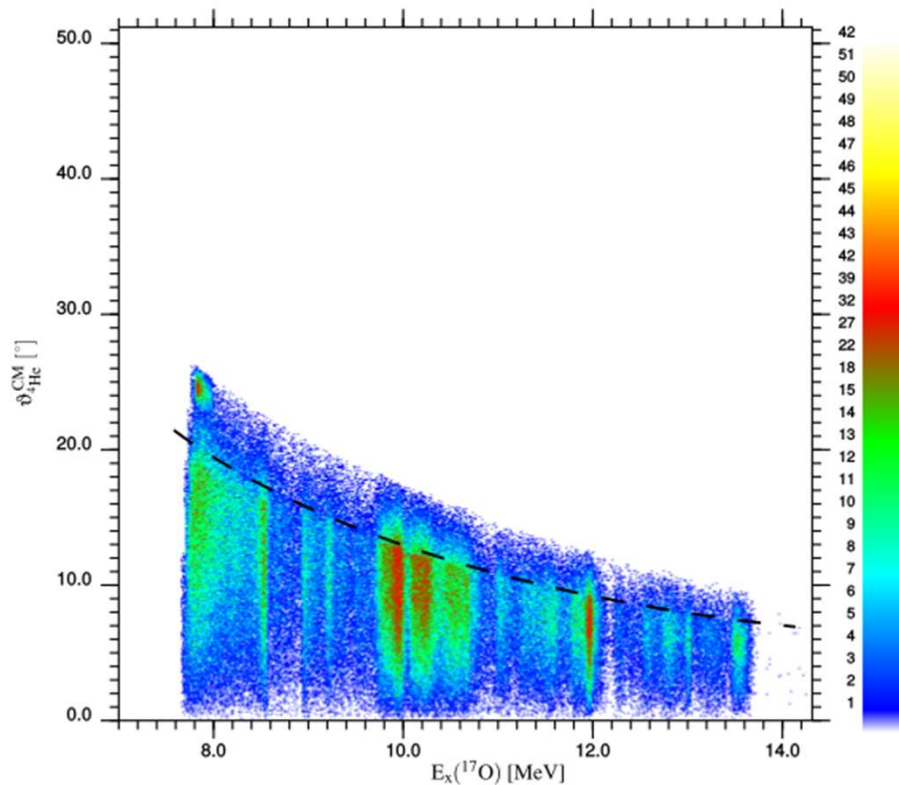
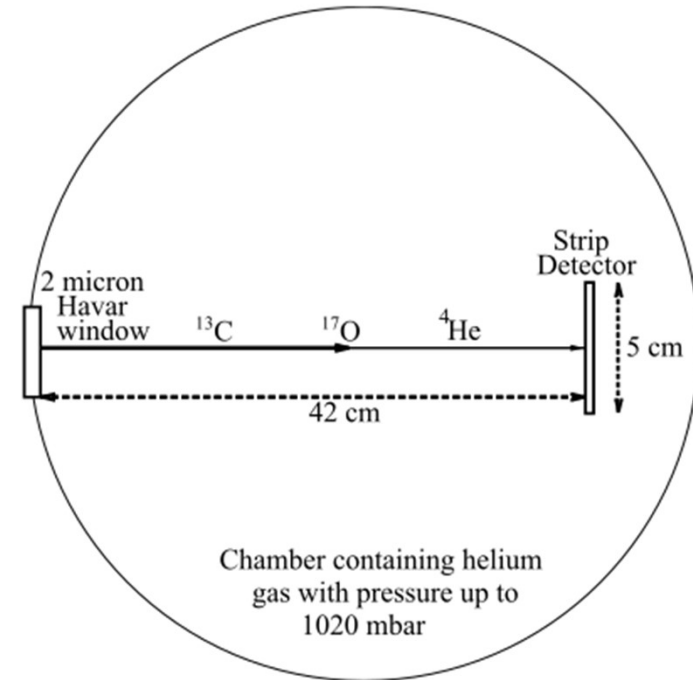
- the resonant scattering  $^{13}\text{C}+^4\text{He}$  experiment and resonant nucleus spectroscopy experiment with the  $^{13}\text{C}+^9\text{Be}$  reaction populated excited states with cluster structure in the  $^{17}\text{O}$  and  $^{18}\text{O}$  (RPSE)
- existing results on the  $^4\text{He}$  decays confirmed and extended
- the  $^6\text{He}$  decaying states in  $^{18}\text{O}$  have been observed for the first time – the first indication of the molecular structure  $^{12}\text{C}-2n-^4\text{He}$
- no  $^5\text{He}$  &  $^8\text{Be}$  decays observed
- these measurements should be complemented with other technique experiments, for example thick target resonant scattering measurements
- further measurements using different techniques are needed to determine the exact value of spin and parity, with higher resolution and statistics to separate nearby states – some of them will be run soon
- there are indications that molecular structure exist in oxygen isotopes but much more experimental data are required

**Thank you !**

# Experiment: Tandem RBI Zagreb Croatia

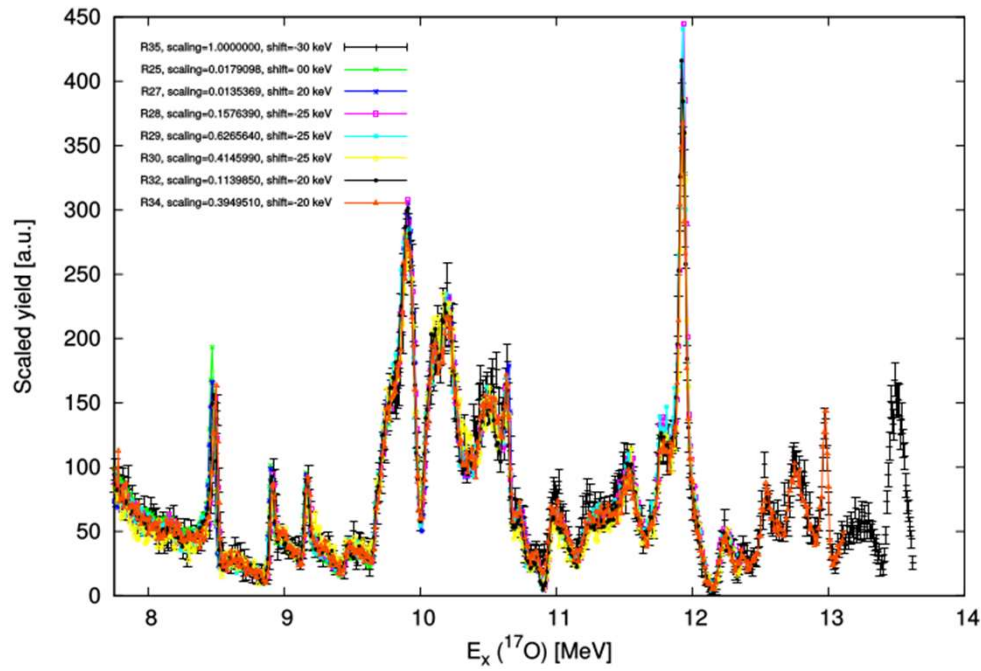
## $^{13}\text{C}+^4\text{He}$ thick gas target resonant scattering

$E_{^{13}\text{C}}$ [MeV]	$p_{^4\text{He}}$ [mbar]	Inelastic-free $E_x(^{17}\text{O})$ range	Run numbers
20.00	312	7.977 – 11.066	25
25.00	461	9.154 – 12.243	27
30.00	591, 589, 587	10.331 – 13.420	28-30, 32
33.00	699	11.037 – 14.126	33
35.00	720	11.508 – 14.597	35



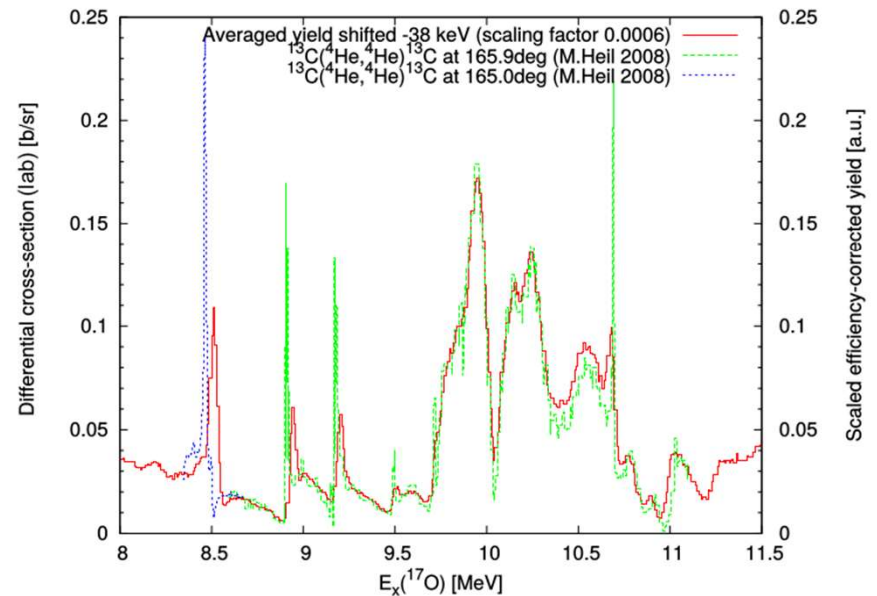
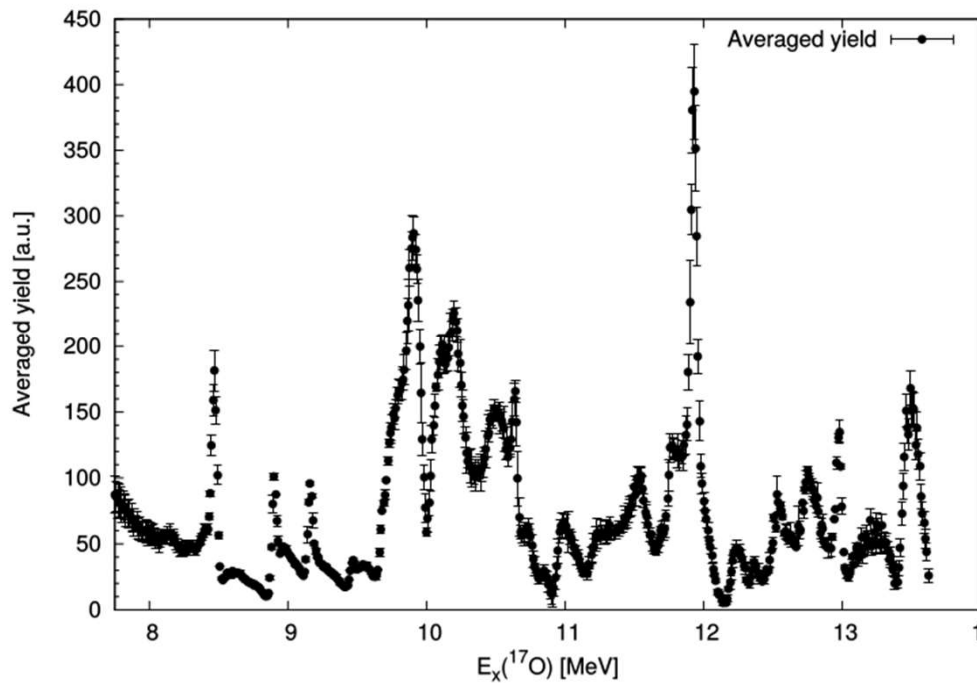
CM angle of scattered  $^4\text{He}$  vs.  $E_x(^{17}\text{O})$   
Assumed elastic scattering

Further steps: detection efficiency correction ( $\Theta_{\text{CM}} < 5$  deg), normalization, data averaging for different runs



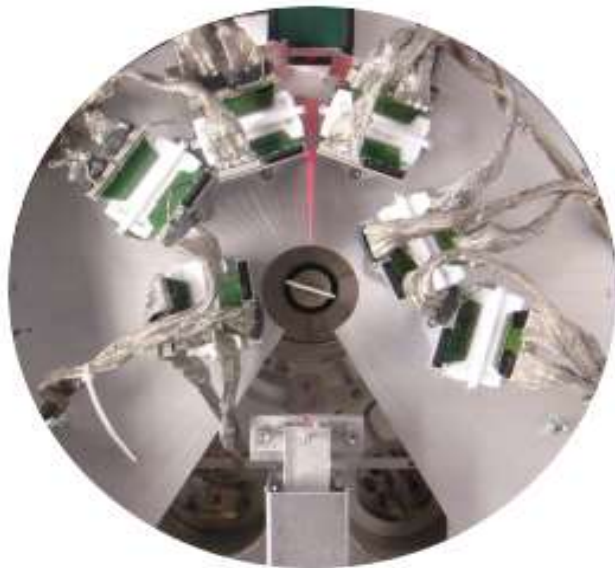
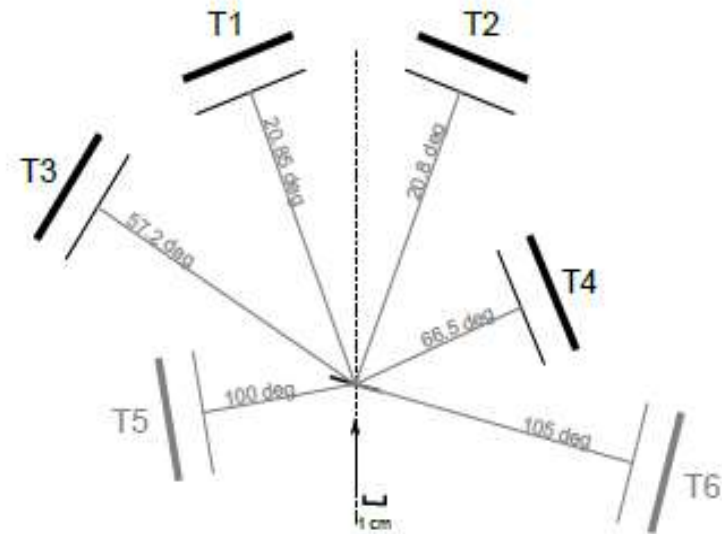
consistent sets of data,  
 inelastic contribution  
 negligible  
 our data at 175 deg

Published data: M Heil et al,  
 PRC 78 (2008) 025803,  
 up to excitation of 11.5 MeV





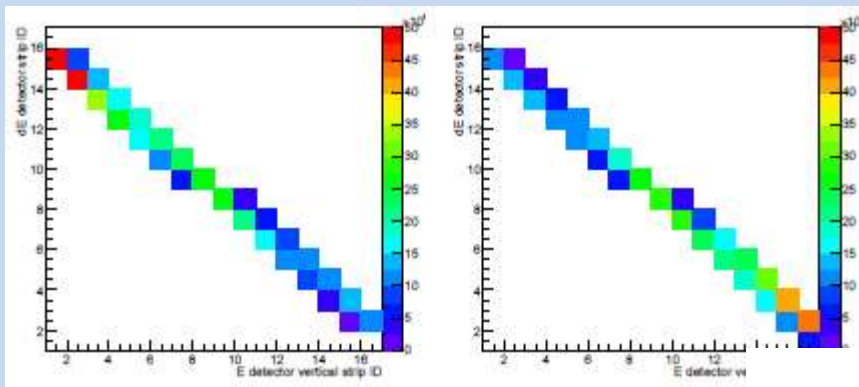
$E(^{13}\text{C})_{\text{beam}} = 72 \text{ MeV}$ ,  $^9\text{Be}$  target thickness  $100 \mu\text{g}/\text{cm}^2$   
 6 telescopes  $20 \mu\text{m}$  SSSD +  $1000 \text{ DSSSD } \mu\text{m}$ ,  $50 \times 50 \text{ mm}^2$   
 Micron Semiconductor type W1



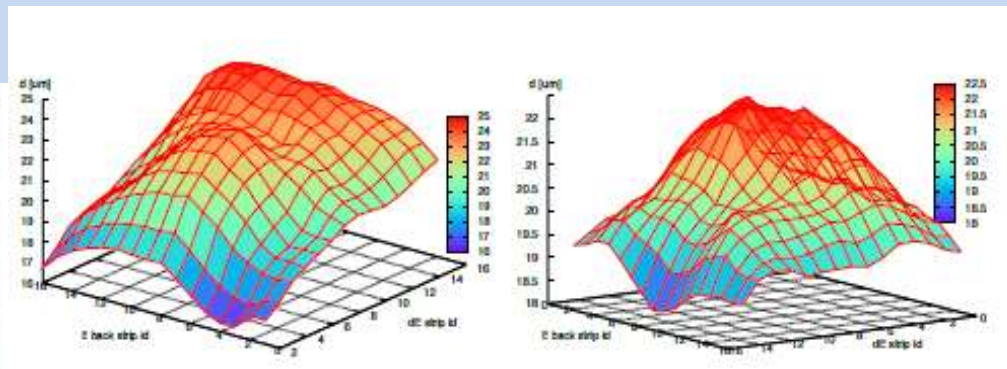
Detector telescope	$\vartheta_{\text{min}}^{\text{in plane}} [^\circ]$	$\vartheta_{\text{max}}^{\text{in plane}} [^\circ]$	$\Delta\vartheta [^\circ]$
T1	11.43	30.30	18.9
T2	11.38	30.24	18.9
T3	48.10	66.31	18.2
T4	52.48	80.53	28.1
T5	83.90	116.10	32.2
T6	95.49	114.76	18.8



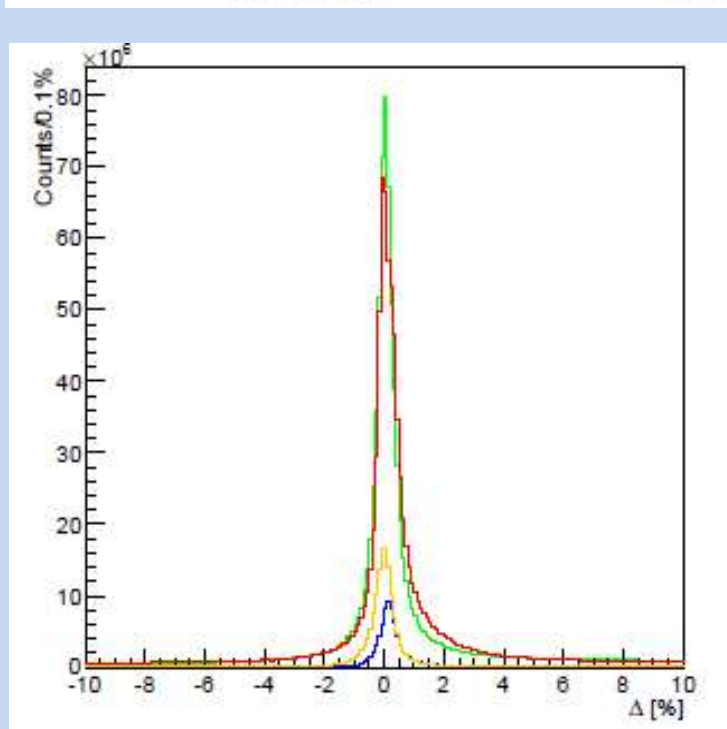
The matching of the  $\Delta E$  (vertical) strips to the E-detector vertical (front) strips



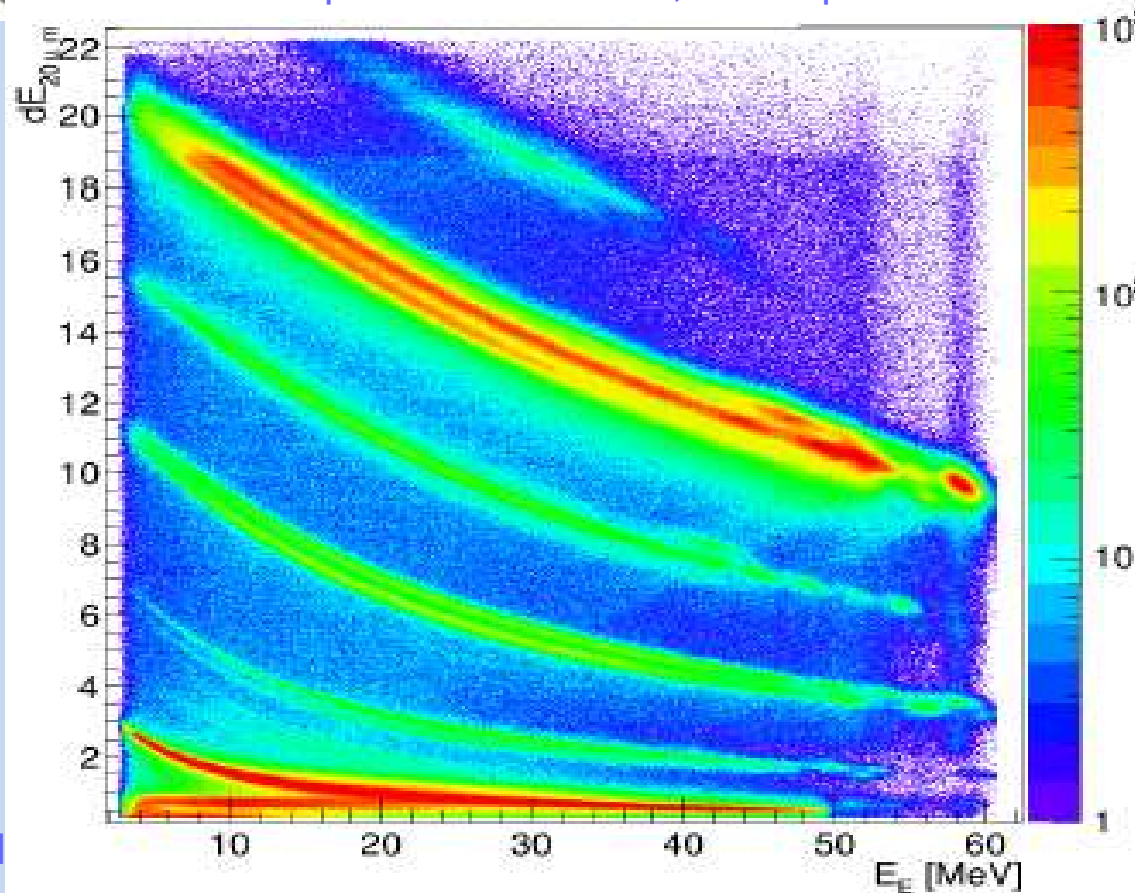
The  $\Delta E$ -detector profiles for the T1 and T2.

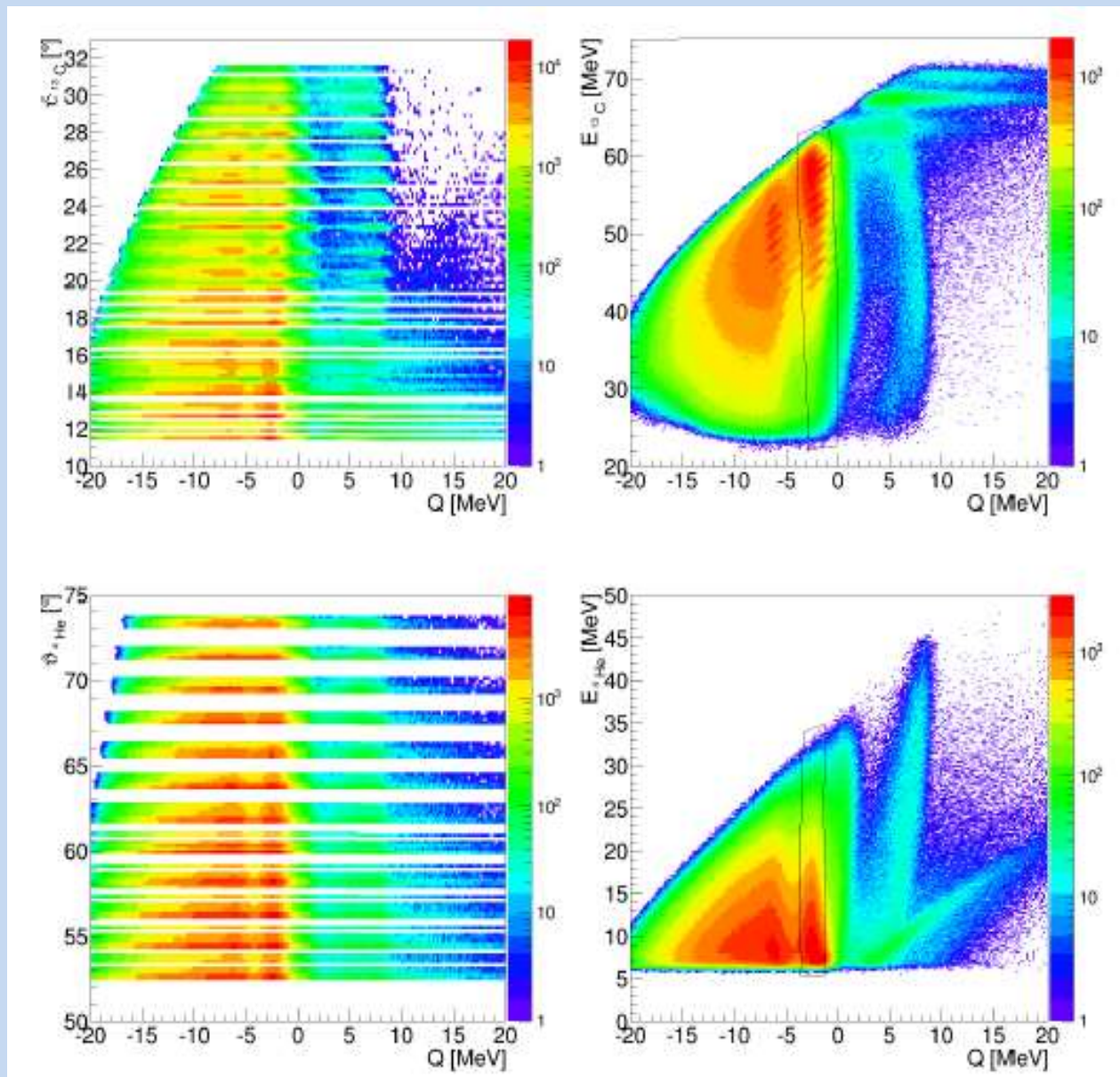


$\Delta E$ -E spectrum for the T1,  $\Delta E$ -strip 13.



The front-strip vs back-strip energy difference relative to the average. Red line T1, green T2, blue T3, orange T4.





The  $\Theta_{\text{det}}\text{-}Q$  and  $E^{\text{det}}\text{-}Q$  spectra for the  $^{13}\text{C}(\text{T1})\text{-}^4\text{He}(\text{T4})$  coincident events. The black line denotes the graphical cuts used to select the ground state reaction channel.